

NORTHWESTERN UNIVERSITY

RAPID VARIATIONS OF BALMER LINE STRENGTHS
IN THE SPECTRA OF Be STARS

A DISSERTATION

SUBMITTED TO THE GRADUATE SCHOOL
IN PARTIAL FULFILLMENT OF THE REQUIREMENTS
for the degree

DOCTOR OF PHILOSOPHY

Field of Astronomy

(NASA-CR-140812) RAPID VARIATIONS OF
BALMER LINE STRENGTHS IN THE SPECTRA OF
Be STARS Ph.D. Thesis (Northwestern
Univ.) 94 p HC \$4.75

N75-11808

CSCL 03A

Unclass

G3/89 53833

Kenneth Bruce McBeath

Evanston, Illinois

August 1974

RAPID VARIATIONS OF BALMER LINE STRENGTHS
IN THE SPECTRA OF Be STARS

Kenneth Bruce McBeath

ABSTRACT

Low resolution photoelectric spectrophotometric measurements of the first four members of the Balmer series in the spectra of one Be and five Be (shell) stars were obtained with the 92-cm telescope and image dissecting scanner at Kitt Peak National Observatory in October, 1972. $H\alpha$ and $H\delta$ were observed simultaneously on two consecutive nights, while $H\beta$ and $H\gamma$ were also observed simultaneously one night before and one night after the $H\alpha$ and $H\delta$ measurements. The time resolution was on the order of one minute, and observations for each star extended continuously over a one to two hour interval.

Equivalent widths were computed for each observation and their standard deviations from the mean values examined by comparing them to the standard deviations for chosen comparison B stars. Results indicate that in three of the program stars, at least one of the Balmer lines shows fluctuations in equivalent width sufficiently greater than those of the standards to be considered real. These fluctuations amount to a few per cent of total line strength and the time scales appear to be on the order of three to thirty minutes. The fluctuations are not always present in a given star, however, indicating that the mechanism producing them may not be continuous.

Power spectrum analysis of the data for the purpose of determining whether the fluctuations exhibit periodicity yielded negative results, and attempts to detect variations in the observed line profiles were unsuccessful because of insufficient instrumental stability.

The noncontinuous and nonperiodic nature of the variations along with their short time scale suggest some form of flare-like or shock origin for the phenomenon.

Approved:

John D. Bahng

TABLE OF CONTENTS

ABSTRACT

TABLE OF CONTENTS.	ii
LIST OF TABLES	iv
LIST OF FIGURES.	v
ACKNOWLEDGMENTS.	vi
1. INTRODUCTION.	1
A. Appearances and Disappearances of Emission Lines, Shell Absorption Lines, or Both	4
B. V/R Ratio and General Profile Variations.	5
C. Changes in Equivalent Width	7
2. OBSERVATIONAL PROCEDURE	9
A. Description of the Instrument	9
B. Specific Parameters for This Research	11
C. Actual Observing Method	12
D. Stars Observed.	15
3. DATA REDUCTION.	17
A. Computation of Equivalent Widths.	17
B. Analysis of Equivalent Widths as Functions of Time. .	19
C. Analysis of Observed Profiles as Functions of Time. .	23
4. RESULTS AND DISCUSSION.	26
A. Existence of Real Fluctuations in Equivalent Width. .	26
B. Periodicity of Real Fluctuations.	31
C. Analysis of Observed Profiles	33
5. DISCUSSION OF INDIVIDUAL PROGRAM STARS.	35
γ Cas	36

TABLE OF CONTENTS (Continued)

49 Per	41
28 Tau.	45
48 Per.	48
59 Cyg.	50
o And	53
6. CONCLUSION.	56
A. Summary and Results	56
B. Comments on Improving the Present Research.	57
C. Suggestions for Further Research.	57
REFERENCES	59
TABLES	63-72
FIGURES.	73-86
VITA	87

LIST OF TABLES

Table

1	Program and Comparison Stars.	63
2	Program Star Block Mean Equivalent Widths	64
3	Comparison Star Block Mean Equivalent Widths.	67
4	Program to Comparison Star Standard Deviation Ratios.	68
5	Lines with Real Rapid Fluctuations.	71
6	Lines with Borderline Rapid Fluctuations.	72

LIST OF FIGURES

Figure

1	Be and Be Shell Hydrogen Line Profiles.	73
2	Line of Sight Orientation for Be and Be Shell Spectrum.	74
3	Schematic Illustration of Image Dissector Principle	75
4	Effect of Low Spectral Resolution on Observed Line Profile	76
5	Scanning Regions for H β and H γ	77
6	Scanning Regions for H α and H δ	78
7	Graph of Equivalent Width Vs Time for 48 Per, H α and H δ , 10 October 1972 (UT)	79
8	Graph of Equivalent Width Vs Time for 28 Tau, H α and H δ , 10 October 1972 (UT)	80
9	Expected Graph of Residual Profiles for a Variable and Nonvariable Observational Line Profile.	81
10	Power Spectrum for 48 Per, H α , 10 October 1972 (UT)	82
11	Power Spectrum for 28 Tau, H γ , 12 October 1972 (UT).	83
12	Effect of IDS Channel Position Instability on Residual Line Profile	84
13	Graph of Residual Profiles for 48 Per, H α , 10 October 1972 (UT).	85
14	Graph of Residual Profiles for 34 Per, H α , 10 October 1972 (UT).	86

ACKNOWLEDGMENTS

The author expresses his deep gratitude to Dr. John D. Bang, who, with his expertise in high time resolution spectrophotometry, ability to teach, and willingness to spend much time helping to find the best methods of attacking this problem, has made this investigation possible. His assistance on the observing run and in the preparation of this dissertation have been invaluable.

My thanks also go to the members of my examination committee, Drs. J. A. Hynek, L. P. Bautz, and W. Buscombe, for their willingness to study the early drafts of the dissertation and to offer helpful suggestions for its improvement.

I especially wish to thank Kitt Peak National Observatory for generously providing not only the observing time for this project, but also the transportation costs from Chicago and room and board during my stay. Special thanks go also to Dr. A. A. Hoag, who spent one full evening instructing us regarding the use of the image dissecting scanner.

I gratefully acknowledge the support of Northwestern University in the form of a four year University Fellowship and several hundred dollars of computing funds, without which this work would have been impossible. The work was additionally supported by NASA grant NGR14-007-122 to Dr. John Bahng.

To Mrs. Mary Jo Simon, for her expert typing of the final draft of the dissertation, also go my thanks.

Finally, a large measure of appreciation goes to my wife, Karen, whose patience, understanding and encouragement during the preparation of the dissertation lightened the loads and made it all that much more enjoyable.

INTRODUCTION

This dissertation is the result of an investigation to detect rapid fluctuations in the equivalent widths of the first four Balmer lines in the spectra of Be stars. This phenomenon, occurring over time periods of less than one hour, represents just one portion of the entire problem of Be star variability. Many different spectral characteristics of these interesting objects have been found to change, and these variations occur over time scales ranging from years down to an hour or less. To understand how rapid fluctuations of equivalent widths fit into this larger picture of Be variability it is necessary to first consider the nature of Be and Be shell spectra themselves and the types of models used to explain them, and then to describe the types of variability exhibited by these stars. The following discussion of the characteristics of the spectra of these emission objects is taken primarily from McLaughlin (1961), Hack and Struve (1971), and Underhill (1966), and is intended only as a summary of the basic information provided by these more complete descriptions.

The typical Be spectrum exhibits hydrogen Balmer lines having central emission peaks superimposed on broad absorption features (the widths of which are proportional to wavelength, suggesting Doppler broadening from rotation). The emission may or may not reach a greater intensity than the continuum, and the profile appears as shown in Fig. 1A or 1B, the latter showing the central absorption core sometimes found in the emission feature, dividing it into two components, violet (V) and red (R). The Be spectrum in all other respects is similar to that of a nonemission B star.

The Be shell stars also show Balmer lines with emission features overlying a broad absorption line. Rather than being a central emission core, however, the emission feature has two rather widely spaced V and R components separated by a deep central absorption as shown in Fig. 1C. The two components are often not of the same intensity, and, as we shall see later, the relative intensities are frequently variable. In addition to the different Balmer emission profiles, the Be shell stars also differ from the Be and nonemission B stars by the presence in the spectrum of several very sharp absorption features due to He I and to ionized metals such as Fe II, Mg II, and Si II. In some cases even the helium and metal lines show emission wings.

The models which purport to explain these phenomena all have their roots in the explanation first proposed by Struve (1931), in which the Be or Be shell star is presumed to be a rapidly rotating B star surrounded by a more slowly rotating ring of gas. As is described below, this model, along with specifications regarding the orientation of the line of sight, can account in general for the Doppler broadening of the absorption features (presumably originating in the photosphere of the star), the presence and profiles of emission features, and the ionized metal features of shell spectra. More detailed information concerning the structure and motions of the circumstellar ring is necessary to account for all the spectral details, but in general the ring model is the one employed in describing these stars.

The differences between Be and Be shell spectra presumably arise from the geometry of the system with respect to our line of sight (see Fig. 2). In the case of the Be profile, the position of the line of

sight dictates that the entire system is seen moving at very nearly the same radial velocity despite the rotation of the ring. Therefore, the emission seen from all portions of the ring will lie very nearly at the center of the underlying stellar absorption line, forming the sharp emission core, the strength of which will depend on the total quantity of gas in the ring and the amount of exciting radiation from the star. If there is sufficient gas between the star and the observer, there may be a small absorption core as shown in Fig. 1B, but one would not expect to find sufficient quantities of intervening gas to produce the helium and ionized metal absorption lines present in the shell spectrum.

In the case of shell spectrum, the ring's rotation is in the direction of the line of sight, so that the emission from the portions of the ring approaching and receding from the observer are respectively blue- and red-shifted with respect to the underlying stellar absorption line. These shifts result in the double absorption lobe profile shown in Fig. 1C. The very deep central absorption is caused by the large quantity of gas in the ring between the stellar disk and the observer. There is also sufficient intervening matter here to produce the helium and ionized metal absorption lines, which are very sharp because of the low pressure in the ring and the fact that the absorbing gas is all moving essentially perpendicularly to the line of sight and hence there is little Doppler broadening arising from the ring's rotation.

All the above described spectral characteristics of the Be and Be shell stars make them very interesting objects, and taken alone would make these stars popular objects for study. Adding even more to their interest, however, is the fact that for very few (if any) of the Be

stars are the spectral features constant with time. Sometimes the variations in the spectra are slow and minor, other times rapid and very striking. The study of Be star variability has a long history, and the following discussion is a brief review of the kinds of fluctuations observed and the time scales involved, in order that the significance of rapid time variations in emission line equivalent widths might be more clearly understood. We shall arbitrarily refer to time scales of years as long, those of months, weeks or days as intermediate, and those of an hour or less as short.

A. Appearances and Disappearances of Emission Lines, Shell Absorption Lines, or Both

This type of change, in which a star develops new or stronger emission or shell absorption lines or in which such lines in a spectrum weaken or completely disappear, generally occurs over a long or intermediate time scale, and has been observed in many different stars, such as γ Cas, Pleione, 48 Lib, and HD 33232 to name just a few examples (Merrill, 1953). Often these spectral changes are accompanied by photometric changes in the luminosity and color index of the star.

The interpretation of this sort of spectral variation is that the shell of gas in which the emission and shell absorption lines originate is being newly generated or has dissipated. The mechanisms for formation are not yet fully understood, and indeed may be different from star to star. Some astronomers feel that the shell formation is the result of the rapid rotation of the star and a resulting slow leakage of material from the equator to the shell, according to Struve's models already mentioned, and in fact there is evidence to indicate that in some instances (Pleione, for example) the shell does form from gas

moving slowly away from the star (Merrill, 1952). Other observers, however, believe that the rotation of the star plays only a minor role and that some eruptive force or other active instability at the stellar surface such as chromospheric radiative outbursts (Underhill, 1960), electric discharges (Johnson, 1955) or a process similar to a solar prominence (Boyartchuk, 1957) is responsible. Here again, some stars, such as γ Cas, appear to have rapidly forming shells following violent outbursts, and so there is evidence for both types of mechanism. There has also been suggestion that, since many of the Be stars are known to lie above the main sequence, the mechanism of origin may be related to an instability developing as a consequence of the restructuring of the star after the exhaustion of hydrogen in the core.

What can be said with relative certainty is that the significance of the appearance or disappearance of emission and shell absorption lines is that the gas rings about the Be star are very often not stable, that they are many times formed and later dissipated, and that most likely there is a variety of mechanisms responsible for these events.

B. V/R Ratio and General Profile Variations

One of the most thoroughly studied of the spectral characteristics of Be and Be shell stars is the ratio of intensities of the V and R emission lobes (V/R) of both the Balmer lines and any ionized metal lines (Fe II, Mg II, Si II for instance) which might also be in emission. It is found that in about 60% of the Be stars this ratio is variable on a long time scale, and about one-fourth of these fluctuations are periodic over about seven years on the average (Copeland and Heard, 1963). Examples of this periodic type of V/R fluctuation are to be found in ζ Tau (Delplace, 1970) and in β Mon (Cowley and Gugula, 1973).

To explain some long term, periodic changes in the V/R ratio, Huang (1973) has proposed a model based on the apsidal motion of an elliptical ring surrounding the star which would seem to explain the phenomenon adequately. Other of these periodic V/R variations, such as in β' Mon, can perhaps best be explained in a binary star model with the secondary being surrounded by an emitting shell which is distended toward the primary and changes orientation during the course of the orbital period (Cowley and Gugula, 1973). A third explanation is offered in the case of ζ Tau, where not only the V/R ratios, but also the emission strengths, widths, and radial velocities change in such a way to indicate a pulsation of the circumstellar envelope which is caused by an instability in the lower regions (Delplace, 1970).

Those variations which are not periodic, on the other hand, pose a different problem. McLaughlin (1961) has attempted their description by calling upon a rotating, irregularly pulsating shell model, but there are quantitative difficulties in this approach which have not been resolved, and the problem is one still requiring explanation.

The V/R ratio in Be stars is also on occasion variable (with little or no accompanying change in equivalent width) on intermediate time scales of a few weeks. This type of variation often occurs in conjunction with the development of or change in a shell spectrum following a violent outburst such as manifested by γ Cas in 1937 (see for example Edwards, 1956). While these variations are not yet explained either, presumably they are connected with the activity producing the shell, or perhaps with revolution about the star of inhomogeneities in the ring itself. Nothing certain is known about these variations, however.

Finally, Hutchings (1967, 1972) has found that the V/R ratio (as well as the overall profile in general) of H β and H γ in γ Cas is variable over a time scale on the order of an hour, a very short time interval indeed. While even less is known about the mechanism responsible for this rapid activity than about the others already discussed, it would seem a safe conclusion that the cause of such a quick fluctuation in these line profiles is not related to changes in the geometrical orientation of the system or any of its parts. It is much more reasonable to suspect that physical conditions in the emitting regions are changing, although nothing more specific can as yet be said.

C. Changes in Equivalent Width

Obviously, in connection with the long term appearances and disappearances of shell spectra, the equivalent widths of the emission and absorption lines both will change, and we will consider variations on this time scale to fall under the first section, which considers shell formation and dissipation. There are equivalent width fluctuations in shorter time scales, however, and these merit separate discussion.

Specifically, the material of interest is evidence from Bahng (1971) that there may be fluctuations in the equivalent widths of H β and H γ in ζ Tauri in the interval of only 10 minutes. If these variations are found to be definitely real in this and other stars, studies of their exact nature and mechanism of origin will provide more interesting clues to the conditions and activity in the systems in which they are present. This present research is an attempt to gather further information regarding this newly studied phenomenon by examining several Be stars to find if it can be observed in them.

If found to be real, what would be the significance of such fluctuations in terms of the Be variability problems already discussed? As in the case of the very quick variations in profiles, it is most likely that the phenomenon is not traceable to geometrical causes, but rather that there is some form of activity actually changing the physical character of the emitting region or the radiation which excites it. Limber (1970) points out that the fluctuation of equivalent widths in ten or twenty minutes implies a volume of activity having dimensions of the order of 1/100 of the stellar radius. An event occurring in this size region may indicate the presence of some flare-like or perhaps shock phenomenon. Further support for this type of explanation is to be found in the belief that electrical discharge, or mechanical or radiative outburst on the surface of the star may be significant in the process of shell formation. If this is true, one can picture the photosphere of a Be star as a very active, unstable environment in which there occur large and small scale outbursts, the latter producing short time scale equivalent width fluctuations and the former producing new circumstellar shells. As it will be shown in the following chapters, the results of this research indicate that the phenomenon of rapidly fluctuating Balmer equivalent widths is real and that the possibility of a randomly occurring flare-like event is certainly attractive, at least qualitatively, as the possible origin.

OBSERVATIONAL PROCEDURE

A. Description of the Instrument

The observations for this research were made on the nights 9-12 October 1972 (UT) at Kitt Peak National Observatory using the No. 2 92-cm telescope equipped with the computer-controlled image dissecting scanner (IDS) designed by A. Hoag, W. Bell and D. Trumbo (1971). The IDS can be used as a rapid scanning spectrophotometer with very good time resolution because it requires no change of the grating position to move from one spectral point to another. Instead, the full spectral image to be observed is placed simultaneously on the photoemissive surface of the photomultiplier, which is surrounded by a magnetic focusing yoke of variable field strength. At a given value of this field strength, only those electrons from a small area of the photoemissive surface (and hence only those from a short range of the stellar spectrum) can reach the first dynode. The rest are deflected and hence ignored by the photomultiplier (see Fig. 3). By varying the strength of the magnetic field of the yoke, therefore, it is possible to select electrons from successive small portions of the spectrum and hence scan the entire spectrum without rotating the grating. It is also possible to scan two noncontiguous spectral intervals without taking the time to cover the interval between by simply making a discrete change in the field strength. This feature is important in the present research because it saves valuable time when scanning the region surrounding two Balmer features while ignoring the interval between them.

In the Kitt Peak IDS the field strength of the yoke, the number of spectral positions to be scanned, the integration time and the recording of output are all controlled by a Honeywell 416 digital computer according to a program prepared by the designers. The program allows the recording of from one to 200 discrete channels of output data, which means, of course, that 200 is the maximum number of data points along the spectral range covered. The spectral resolution and separation of these points will depend upon the specific grating and spectral order used in a given project, and those for this project are presented below.

The purpose of a rapid scanning spectrophotometer is to integrate over the entire spectrum as quickly as possible and then keep repeating this procedure as many times as required, adding the results of each scan to the total in order to obtain a statistically reliable total number of counts per channel in the final spectrum. In this way, the effects of changes in seeing and transparency are effectively eliminated by smoothing them out over the many individual scans which have been added together to give the final spectrum. In this work, a single integration of the spectrum will be called one scan, and the final total of several scans which is recorded when the number of counts in each channel is sufficiently large will be called one observation.

The program for the Kitt Peak IDS allows a minimum integration time of one millisecond per channel (with a dead time between channels on the order of 2%). The total time to integrate once over a given spectrum will depend of course on the total number of channels used, but even at the maximum of 200 the time is 0.2 second, which is much shorter than in scanners with movable gratings.

The IDS system at Kitt Peak also provides a storage oscilloscope display of the counts in all 200 channels as they are being recorded. This enables the observer to view the spectrum while integrating in order to be sure that the system is working properly, that a reasonable number of counts is being accumulated and that the spectral features he desires to measure are in fact centered in the channels being scanned.

B. Specific Parameters for This Research

Below are listed several of the physical parameters which determined the spectral and time resolution of the observational data in this research project.

Entrance aperture: The aperture of the spectrometer was circular with a diameter of 6 seconds of arc when projected on the sky.

Grating: In the spectrometer, a 300 lines/mm grating which yielded a reciprocal dispersion of 60.5 Å/mm in the second order was used.

Resolution: With the dispersion given above, the physical size of the area of the photocathode examined in any one time by a given channel (called the slot width) resulted in a spectral resolution of 20 Å in the second order and 40 Å in the first.

Step size: The step size between successive channel centers was 4.27 Å in the second order and 8.54 Å in the first.

Spectral coverage limit: In second order a maximum of 880 Å coverage was possible at any one grating position.

Photomultiplier: An ITT F4011RP S-25 photomultiplier was used in the IDS in order to achieve adequate red sensitivity

to measure H α . The tube did not require cooling because in an image dissector at any given moment, the effective cathode area, from which any dark count must come, is equal to the slot width, which has dimension of 0.3 mm. An area of this size yields only about 6 counts/second of dark count, much less than the expected statistical noise of approximately 100 counts/second/channel.

A word should be said here regarding the effect of the low spectral resolution of the scans on the observed profiles of the lines. Any structural details such as emission lobes or central absorption cores are invisible in the final observed profile, as shown in Fig. 4, in which the true profile for H α in μ Per as measured by Gray and Marlborough (1974) appears above a sample observational profile of the same line from the IDS data. One can see that the exact profile of the line is completely lost, and that the observed profile will include the entire stellar absorption line as well as the emission feature. It is true, nevertheless, that equivalent width measures are not affected by the loss of resolution, and hence the system is suitable for the measurements desired here.

C. Actual Observing Method

Although seven nights of telescope time were originally allocated for this observing run, the first three were lost because of poor weather. On the first clear night observations were made with the grating positioned to scan H β and H γ . On the second night the grating was moved to cover H α and H δ , to insure observations of all of the first four Balmer lines in case the weather should again prove unfavorable. Fortunately, the third and fourth nights were also clear, and

$H\alpha$ and $H\delta$ were again scanned on the third while $H\beta$ and $H\gamma$ were repeated on the last night of the run. The result then was four nights of observations evenly divided between the two pairs of Balmer features. It became impossible to make the additional intended observations because soon after this run the instrument was dismantled.

On each night the two lines in question were observed simultaneously in each star. In the case of $H\beta$ and $H\gamma$, both lines were observed in the second order, the scans being made over 31 data channels centered about $H\beta$ and then skipping to 31 channels centered about $H\gamma$ (see Fig. 5). For the $H\alpha$ and $H\delta$ observations, however, the separation of more than 2450 Å between the line centers prevented the two lines from being placed simultaneously on the photoemissive surface of the IDS in the same spectral order, since the second order spectral coverage limit was approximately 900 Å as mentioned previously. It was possible to observe $H\alpha$ and $H\delta$ at the same time, however, by sacrificing a factor of two in spectral resolution for $H\alpha$ and observing it in the first order while observing $H\delta$ in the second. $H\alpha$ in the first order falls at the same location spatially as λ 3282 in the second order, which is close enough to $H\delta$ (λ 4101) to be studied at the same time. The procedure was to insert a GG 13 filter in the spectrometer to block light of wavelength shorter than 3800 Å so that there would be no second order spectrum overlapping the first order $H\alpha$ line. Because of the low sensitivity of the S-25 photomultiplier to near infrared radiation of λ 8200, and the low amount of continuum radiation of B stars at this wavelength, there was no problem of first order contamination of the second order $H\delta$ line. The scans then were made through 31 data points centered on $H\alpha$ and then skipping to 31 points centered about $H\delta$ (see Fig. 6).

The exact 31 channels which included each line were found at the beginning of each night by using all 200 channels to scan the spectrum of a star with obvious hydrogen Balmer lines and viewing the results on the storage tube display. From this display one could easily determine which channels included the proper spectral regions, and these were then programmed for the night's observations.

Thus for both pairs of lines there were 62 data channels per scan. The system was operated at the minimum integration time per channel; each scan therefore required a total of 62 milliseconds. The total number of scans for each observation had to be determined separately for each star on each night. The goal was to accumulate a minimum of 10^4 counts per channel, since at this level, the statistical fluctuation is at most one percent. The number of scans necessary to reach this level depended on the apparent magnitude of the star and the transparency of the atmosphere. The transparency was quite variable even over the course of one night because of the presence of moving thin cloud cover, but since this type of obscuration does not affect equivalent width measures, it was necessary only to increase the total integration time (i.e. the number of scans) to receive a sufficient number of counts. Similarly, extinction arising from zenith distance changes have no effect on the measured equivalent width, hence no special corrections were necessary. The extreme values of scans necessary were 500 and 2000, so that the total time for single observations ranged from 31 to 124 seconds. The most common total integration time per observation, however, was 62 seconds (1000 scans).

At the end of each observation the computer automatically recorded all the data on magnetic tape, a process which required only

about one or two seconds, resulting in very nearly continuous observation of the stellar spectra. The data which were recorded after the completion of each observation included the following:

1. The identification number of the observation (beginning at one each night and running sequentially throughout the night),
2. The UT starting time of the observation to the nearest second,
3. The number of counts recorded for each of the 200 channels available in the system (obviously, any not used would be recorded as 0), and
4. The number of scans in the observation.

Such data as the star identification, lines observed, notation of sky conditions, and so on were recorded manually on a separate log sheet.

The order of observations for a given program star proceeded as follows: Five observations were made of a comparison star which had been chosen specifically for that program star (see next paragraph). Then the program star was observed for a period of from one to two hours, and then finally another five observations of the comparison star were made. During the program star observations the centering of the stellar image in the entrance aperture was maintained by continuous monitoring of a guide star through the offset guiding eyepiece on the instrument.

D. Stars Observed

Table 1 gives the program stars for this project as well as the comparison star for each. The comparison stars (early B stars showing no emission) were chosen to be in fairly close proximity to the program

star for which they were used. It is assumed that the equivalent widths of the Balmer lines in these stars were constant over the observed time scale of a few minutes so that their measures can be used as a determination of the stability of the system and its ability to detect small fluctuations in equivalent widths at the low spectral resolution used.

DATA REDUCTION

All the numerical computations for this research project were performed on the CDC 6400 computer system of Northwestern University's Vogelback Computing Center.

A. Computation of Equivalent Widths

The computation of the equivalent width measured for each line at each observation was begun by extracting from the 200 data channels only those actually scanned (31 per line). For each line the number of counts in each channel was normalized to the value in the first channel. These values were then used to establish the position of the continuum. The procedure for this computation was to assume for the first attempt that the eleven central points of the scan lie in the spectral line, and so these points were at least temporarily ignored, leaving ten points at each outside edge of the scan region which were assumed to be the continuum. The least-squares solution to the best straight line through these twenty values of (i, N_i) , where N_i is the normalized count value in the i^{th} channel, and the corresponding value for the standard deviation from this line (σ) were computed.

For all 31 channels, the normalized value of each was compared to the continuum value just calculated. If the difference of the two exceeded 2σ , the point was considered to lie not in the continuum but rather in the line. If the list of such channels included any points other than the central eleven, or if any of those central points were not included, the continuum calculation was repeated using the new list of points considered not to lie in the line, calculate a new value

of σ , and then look for points lying more than 2σ away from the new line. This iterative procedure would continue until one of two conditions was satisfied. If from one calculation of the continuum to the next there was no change whatsoever in the lists of points included in the calculation and those excluded as being in the line, the process would be terminated and the continuum considered to be accurate. Alternatively, the fifth continuum would be considered final even if the first condition were not satisfied. The purpose here was to allow for the possibility that the scatter in an observation might be sufficiently great that even when the continuum was accurately placed there may be two or more points of the continuum on opposite sides of the line and at a distance greater than 2σ from it, hence preventing the first condition from ever being satisfied. It was determined that the method described would accurately place the continuum in less than five iterations if the scatter were not a factor, and so the limit of five iterations was imposed. In practice it was found that only 45% of the observations required the full five iterations to fix the continuum level, and for each observation in that group there were only one or two points of the continuum beyond the 2σ limit.

Once the continuum level was determined the equivalent width of the line was calculated numerically in the customary manner using the points not used in the final iteration of the continuum calculation. To reduce the possibility of including erroneously a "noisy" continuum point not eliminated by five iterations, none of the first or last eight points of each line were used in the equivalent width calculation, even if more than 2σ from the continuum. These points were known after examination of many observations to lie beyond the wings of the line.

At this point, a check was made to determine whether equivalent widths derived in this manner for the comparison star spectra were in fact constant by examining the observations of these lines to see how much noise was present in the data. For each block of five observations of a comparison star a mean value and a probable error of a single observation were computed, and then all of these probable errors for all the stars were averaged. It was found that this average probable error for a single observation was 0.16 Å (the full range in values was from 0.05 to 0.25 Å), and so it appears that the procedure adopted is capable of measuring the equivalent widths of the lines to an internal accuracy of 0.2 Å.

It is of course possible that the above method will introduce a systematic effect into the values of the equivalent widths, but as the intention is only to compare successive observations looking for fluctuations, such an effect would be unimportant in this research project.

At this stage then equivalent width values for the two spectral lines in each observation and the time of each observation were known.

B. Analysis of Equivalent Widths as Functions of Time

The CDC 6400 was used with the Calcomp plotter to produce graphs of the equivalent widths as functions of time. Lines observed simultaneously were plotted together. Results of two typical plots are shown in Figs. 7 and 8. The data across the center of the plot include HR number of the star, and the date and starting UT for the observation. It soon became obvious that visual inspection of these graphs would not be sufficient to decide upon the reality of fluctuations in equivalent widths, and the decision was made to perform the analysis entirely

numerically. The analysis was performed separately for each night's observation of each star.

For each individual line, a mean of the equivalent width values was calculated and, using this, a value for σ , the standard deviation from the mean according to the formula

$$\sigma = \sqrt{\frac{\sum_{i=1}^n (w_i - \bar{w})^2}{n - 1}}$$

where w_i is an observational value of the equivalent width, \bar{w} the mean value, and n the total number of observations. A mean value and σ for the five observations of the comparison star preceding the program observations and separately for the five following them were also computed. The comparison star observations before and after their respective program stars were kept separate so as to be able to detect any possible change in the stability of the system over the course of the program star observations.

It should be noted that the standard deviation from the mean of a series of quantities is independent of the total number of observations (a fact not true for the more familiar standard deviation of the mean $\sigma' = \sqrt{\sigma^2/n}$) and so the fact that there are only five observations in each comparison star group and from 60 to 200 in the program star runs does not invalidate any comparison between the magnitudes of the standard deviations from the mean of the program star, σ_p , and of the comparison star before and after the program observations, σ_{c1} and σ_{c2} .

Such a comparison was in fact used to determine the reality of fluctuations in the equivalent width values. The criterion established for the existence of real fluctuations in a given Balmer line strength was that the following condition be satisfied for that line:

$$\frac{\sigma_p/\sigma_{c1} + \sigma_p/\sigma_{c2}}{2} \geq 2.0$$

The goal was to find fluctuations with standard deviation from the mean twice as great on the average as those which were attributed to noise of the system. In these cases the line strength variations would be considered real.

In addition to deciding if the fluctuations in measured values were real it was desired to determine if they might be periodic, and so at this stage the individual values of equivalent width and the times of observation were submitted to a power spectrum analysis performed by a library program of the Vogelback Computing Center. The program uses the Cooley-Tukey algorithm for performing the Fourier transform involved and makes a rapid determination of periodicity possible. Since the program requires that the input data points be uniformly separated in time, some program star observations which were interrupted by clouds or mechanical delay were divided into smaller groups treated independently to preserve a uniform time interval.

In addition to the program data, test data of known period and amplitude were also processed for the purpose of calibrating the amplitude of the periodic wave input in terms of the power at a given frequency peak in the power spectrum. The resulting calibration was determined to be

$$a^2 = \frac{1}{0.15} A_p \cdot \Delta f$$

where a is the semi-amplitude of the sinusoidal variations at a frequency f in the original series of observations, A_p the height of the peak in the power spectrum at frequency f, and

$$\Delta f = \frac{S}{2B}$$

In the expression for Δf, S, the sampling rate, is the number of observations per minute; and B, the number of frequency bands, is the number of discrete frequencies resolved by the power spectrum analysis. B is an increasing function of the total number of observations in the sample. This calibration was then to be used later to determine the magnitude of any periodic variations found.

As will be discussed in the next chapter, the results obtained from the power spectrum analysis were not very striking, and so two different procedures were followed to be sure that indeed no periodicity was present. First, the power spectra for both nights' observations of any line determined to be variable were averaged (each night weighted according to the total number of observations) in an attempt to smooth out the noise and emphasize any frequency peaks. The other procedure was to take a single night's observations and average each successive pair of points before performing the power spectrum analysis. While of course cutting the number of data points in half, this procedure would also smooth out noise and emphasize peaks.

C. Analysis of Observed Profiles as Functions of Time

In addition to the measurements of equivalent widths described above, the observed profiles of the lines were examined to see if any changes could be observed there in connection with the equivalent width fluctuations. As mentioned earlier, with our low resolution of 20 Å (or 40 Å in the first order), the profiles obtained were greatly broadened and any internal details such as violet and red emission lobes were not visible. It was thought possible, however, to investigate whether there would be some visible effect in the observed profile if the actual line profiles were changing.

To begin the examination of these profiles each night's observation of each star was taken separately. Since the intention was now to examine successive profiles of these lines, it was necessary to be sure that the profiles were always fixed with respect to the data channel position, an unnecessary condition when we considered only equivalent widths. Now in principle one would expect that once programmed, the 31 data channels positioned around a given line would be fixed with respect to wavelength, meaning of course that from observation to observation a given channel would always contain exactly the same wavelength interval. In practice, however, it was found that there were two possible causes for the wavelength position to shift slightly with respect to the data channel position.

First, if the star image should move in the entrance aperture in the direction of dispersion, then the spectrum would shift in the same direction and the displacement in channel position would occur. Such a change in image position could be due either to faulty telescope tracking or from movement of the image within the seeing disk. In the

second order, to cause the spectrum to shift by one full channel an image position drift over an angle of approximately $2''$ in the proper direction would be required. Since the telescope was continuously guided it is felt that the amount of drift from telescope tracking error was never as large as this angle, but the seeing disk on the four nights of the run was on the order of $2''$, and so channel drift from this cause cannot be ruled out.

The other possible cause for channel drift was instability in the voltage applied to the deflection yoke. With 200 channels available, a fluctuation of 0.5 percent would alter the wavelength position by one full channel. Since this possibility also cannot be easily ruled out, it was decided to check for channel shift before comparing successive observed profiles. This was accomplished by examining the 31 channels surrounding the line, finding the maximum or minimum count value (depending on whether the line was in emission or absorption), and adopting this channel as the line center. The profiles were then artificially shifted so as to place this central point in the same channel for each observation.

Now a mean profile was computed by averaging the number of counts in each channel over all the observations. Then each profile was compared to this mean by computing the percentage deviation of each channel from the mean for that channel (Resid_i).

$$\text{For channel } i: \text{Resid}_i = \frac{c_i - \bar{c}_i}{\bar{c}_i}$$

where c_i is the number of counts in the channel. Finally, for each observation of the line the mean Resid over all the channels in the

line was subtracted from each Resid_i . This was done to eliminate the effects of a change in atmospheric transparency which would produce large values of Resid_i for all of one observation but would not alter the shape of the profile from that of the mean profile.

The results of these calculations were then plotted graphically. What one would expect to see in the cases in which a line was, and was not, showing fluctuations from the mean profile is illustrated in Fig. 9.

RESULTS AND DISCUSSION

A. Existence of Real Fluctuations in Equivalent Width

If we define one night's continuous observations of a single Balmer line in one program star to be a block of observations, then there were 38 blocks completed over the four-day observing run, each consisting of from 60 to 200 observations of an equivalent width. The differences in lengths of the blocks arises from the differences in time resolution (from brightness differences in the stars) as well as the necessity of shortening some so as to be able to observe all of the program stars desired in the available dark hours each night.

Table 2 gives the line identification, data, number of scans per observation, number of observations, mean equivalent width for each block, and if available a published value of the equivalent width from the literature for the purpose of comparison to help judge the performance of the IDS and the reduction procedure. An inspection of this information reveals that the mean equivalent width values are not greatly different from published values and are very consistent from night to night. The largest differences between two successive mean values for the same line is 0.5 Å, and the average difference for all the blocks is 0.2 Å, an indication that over a long time base the IDS performance was stable. Mean values for the equivalent widths of the comparison star lines, and published values, are given in Table 3, and here again the consistency is quite good.

The data found in Table 4 are those used for the determination of the existence of real fluctuations in these equivalent widths. The first four columns give the star, the line in question, the date, and

then the standard deviation from the mean (σ_p) for that block's observations. Following these columns are two which give the standard deviation from the mean of the comparison stars as measured before (σ_{c1}) and after (σ_{c2}) the program star block. The last column of Table 4 gives the average value of the ratio of σ_p to σ_{c1} and σ_{c2} . It is this number, as described in the previous chapter, that must equal or exceed 2.0 for the fluctuations of the equivalent width to be judged real. Examination of the table shows seven blocks for which the criterion is satisfied, and the star, line, and date for each are listed separately in Table 5. The last column in this table is included to show the approximate percentage change in line strength occurring during the fluctuations. The quantity given is $\frac{\sigma_p}{\bar{w}} \cdot 100$, where \bar{w} is the mean equivalent width for the block. Since the root mean square deviation is equal by definition to $\sqrt{\frac{n-1}{n}} \sigma_p$, this given quantity very closely approximates the r.m.s. percent deviation of the equivalent width. The matter of time scales for the variations will be discussed later.

From the data thus far presented the following points are noted regarding the existence and nature of variations in the equivalent widths of Balmer lines in these program stars:

1. In seven blocks (belonging to three of the six program stars (η Per, 28 Tau, 48 Per)), it would appear that in fact, real variations in the line strengths are occurring over the time period of the observations. These seven cases can actually be divided into two separate groups. The first group, consisting of H α in η Per and 48 Per, and H β in 28 Tau, are three lines which have a reasonably large equivalent width, and the variations therefore are a small percentage

of the total line strength. With lines of these intensities, any error with small absolute value in the placement of the continuum would result in a very small percentage error in the equivalent width because of the large separation between line and continuum.

In the case of the other group (the remaining variable lines), however, the equivalent widths are very small (absolute values less than 2.0 Å). While the numerical method of continuum placement used is intended to be purely objective, it is of course probable that when the line profiles lie so very close to the continuum, a few points of the line will be included in the computed continuum, and there may be small errors in the continuum placement which, by virtue of the weakness of the lines, could represent a sizeable percentage of the total strength and lead to a spuriously high value for σ_p . So, while it is not possible to make a quantitative statement regarding the confidence in the results of the two separate groups, it is the feeling that the variations of the first group are more reliably established than for the second, although all are still considered real. Presumably the large apparent percentages of variation found for this second group are in reality on the order of only a few percent, the difference being attributed to computational difficulty with the weak lines.

2. In three more blocks, which will be called borderline cases and are listed in Table 6, although the criterion for establishing the presence of fluctuations is not satisfied, either σ_p/σ_{c1} or σ_p/σ_{c2} taken alone was actually greater than or equal to 2.0. This may in fact be just a noise effect, or might possibly indicate that at the beginning or end of the block there were variations occurring which were not present throughout the entire time period covered by the block. More extensive observations would be required to decide the question.

3. Since the fluctuations occur in both Be (48 Per) and Be shell (28 Tau and α Per) spectra, increased support is found for the belief that the origin of the fluctuations is unrelated to the line of sight geometry but is intrinsic to physical characteristics of the star-ring system.

4. In only one case (if one disregards the borderline case of H α in 28 Tau) are the fluctuations of a line found on both nights the line was observed. The significance of this fact lies in the support it lends to the suggestion of flare or shock phenomena as the mechanism of origin, since this sort of mechanism would not necessarily be operating continuously, and one could expect to have periods of low activity.

5. In no case (again not considering borderline cases) are two different spectral lines measured simultaneously both found to be variable at the same time. The obvious conclusion from this fact is that whatever the mechanism of origin for these variations, it does not operate to the same degree on all of the Balmer features, but rather on one (or, of course, perhaps more than one which are not measured) more strongly. Sometimes it is the higher series member of the two which varies, sometimes the lower. This feature of the variations may imply a stratification according to excitation level of the shell, and a disturbance which moves through it, causing different lines to fluctuate at different times.

Regarding the time scales of these variations the following can be said. As will be pointed out in detail in the section describing the results of the power spectrum analysis of the data, no periodicities were found. This fact makes the determination of the exact

time scales of the real (and random) fluctuations rather difficult, because the standard deviation from the mean tells nothing of how frequently the data are varying, only the amount of the average variation. It is possible to place limits on the time scales, however, based on the time resolution and lengths of blocks.

Since three observations during the course of a variation are necessary for detection, a time resolution of approximately one minute implies that the minimum time scale variation that could possibly be detected in this analysis must be at least three minutes. Any shorter time scale would be missed, unless by chance the observations coincided with the times of extreme values, an unlikely event.

On the other hand, for fluctuations to be detectable in observations over a specified time interval, it is necessary for that interval to extend over at least two or three cycles of the variation. In the present case, in which the variations were detected in blocks of approximately one hour in length, this restriction implies an upper limit to the time scale of 20 to 30 minutes. This upper limit could actually be much larger if in fact the equivalent widths were changing monotonically over a relatively long time scale, but inspection of the equivalent width graphs as functions of time indicates that this is not the case. There is no net slope of the data, only scatter about the mean, which would indicate that the time scale of the detected variations must be on the order of a few minutes rather than close to an hour or longer.

The conclusion is, therefore, that the observed fluctuations are occurring over time periods of from three to 30 minutes, and that from this data analyzed in this manner it is not possible to fix the duration of the variations more precisely.

B. Periodicity of Real Fluctuations

As was briefly mentioned in the previous chapter and the above section, the results of the power spectrum analysis of the equivalent width data were negative. The first analysis of the raw data produced power spectra such as those in Figs. 10 and 11. Figure 10 shows the power spectrum for H α in 48 Per on the night on which it was variable, and Fig. 11 shows the power spectrum for the constant H γ line in Pleione. At first glance it might appear that there are a few peaks which would indicate periodic components to the fluctuation. Inspection of three features of the power spectra show this to be untrue, however.

First, in the power spectra of the variable lines, the peaks which do appear have very small numerical value, and when one applies the established calibration equation (given in the chapter on Data Reduction) to their values one finds the amplitude indicated for the actual periodic wave is consistently only one-third to one-half the value of the standard deviation from the mean. If the fluctuations were periodic the amplitude of the wave should identically equal the amplitude of the variation, since they would be one in the same. The observed peaks must therefore be noise.

Secondly, the peaks are only on the order of two or three times the general noise level in the power spectra and, since the peak height is proportional to the wave amplitude squared, any periodic wave would have an amplitude greater than the noise by less than a factor of two, which is not a significant amount and does not indicate the definite presence of a periodic variation. It is of course quite possible, because of the coarse frequency resolution of these power spectra, that an actual frequency peak lies between the highest two points in the

power spectrum and is in fact farther above the noise than appears from the output. Again, however, because of the peak's proportionality to the square of the wave's amplitude, it is unlikely that even if computed from actual peak height values (which are not expected to be vastly different from the values used), the resulting wave amplitudes would sufficiently exceed the noise levels to be considered real periodicity.

Finally, there are no striking differences between the power spectra of those lines judged to be varying and those which are not. This fact implies that there is sufficient noise in the data to create small peaks in the power spectra even when the line is not actually varying. (As yet another check on the performance of the IDS we note that these peaks are numerous, small, and close to the noise level in blocks where no variation is present, and conclude that there is no periodic noise source in the system.)

In order to be absolutely sure that no periodicity is present in these data, we performed the two averaging processes described in Chapter 3. If a weak periodicity were present, one or both of these techniques might suppress the noise and emphasize the power spectrum peak. Both led to negative results again, however. The general noise and peak levels remained the same, and as in the raw data analysis there were no peaks significantly above the noise. Our final conclusion therefore is that the observed fluctuations are completely random.

In many ways this result is a very reassuring one. First, since geometric origins for the variations are considered unlikely, periodicity from these causes is not to be expected. Secondly, as has been noted, it is the author's feeling that a flare or shock

phenomenon is responsible for the presence of the short time scale fluctuations. If this is indeed the case, the existence of a periodicity in those variations would be a rather difficult phenomenon for which to account, since one would expect that flares or related activity would occur at random intervals, especially on a time scale such as is being considered. So the failure to detect periodicity is considered supportive to the idea that the line strength fluctuations are originating in small areas and caused by random, flare-like activity.

C. Analysis of Observed Profiles

This part of the analysis proved to be much more difficult than first imagined. The real problem lies in the elimination of channel position shift, which has been described earlier. The expected effect of unremoved channel shift is shown in the two parts of Fig. 12. The left half of the figure shows an individual profile which is identical to the mean profile except that it has been shifted slightly to the left. The right half then shows the resulting graph of the residuals from the mean computed as described in the previous chapter. The characteristic "s" shape is very distinctive. Figures 13 and 14 show some actual graphs of these residual profiles for the observations, and one sees immediately that the same "s" shape is quite commonly present both in the variable H α and constant H δ lines in 48 Per and the constant H α and H δ lines in the comparison star 34 Per. The obvious conclusion then is that image drift within the seeing disk, instability in deflection yoke voltage, or both, are working to change the spectral position relative to the data channels, and the attempts to remove the shift numerically have been unsuccessful. Apparently the shift in

position is not an integral multiple of channel width, since this method of removing shifts is capable of moving the data in integral channel units and would presumably have succeeded in such a case. Hence it is impossible to eliminate these partial shifts between observations.

Because the "s" shaped residual profile is the only kind which is found in any block of observations, the necessary conclusion is that if there are any profile fluctuations occurring in conjunction with the changes in equivalent width, they are undetectable with this system. Its coarse spectral resolution and apparent instability in channel position preclude any such profile examination.

DISCUSSION OF INDIVIDUAL PROGRAM STARS

The purpose of this chapter is to present a summary of the observed characteristics and spectral history of each of the six program stars studied in this research project in order to determine their similarities and differences and to see how the present investigation and results are related to the previously accomplished research on these objects. Since studies of equivalent width with time resolution of only a minute are extremely new and results are in general unpublished, it is not possible to compare the results obtained here to those found by other observers, but they can be considered in the light of the introductory chapter's discussion of Be star variability and its interpretation.

γ CAS HD 5394 HR 264

Published Spectral Types	References
B0 ne	40
B0 IV: e	8, 9, 46, 60
B0 IV	11, 62, 66
B0 IV p	59, 76
B0 IV pe	44, 48, 75
B0 IV pe (sb)	63

Published <u>V sin i</u> (km/sec)	References
300	2
310	12

General Spectroscopic Appearance

Except for the period from approximately 1932 to 1942, which will be discussed in great detail in the section concerning spectral variations, the spectrum of γ Cas has been that of a reasonably stable Be star. The first few members of the Balmer series show emission in two components with a central absorption core, all of which overlie the usual broad stellar absorption feature. There is also faint emission at the stronger lines of Fe II, Mg II, and at times the helium D_3 line. When photometry or spectrum gradient measures are taken, one finds that the star has an infrared excess, which is at least in part traceable to the presence of Paschen continuum emission in the spectrum (Andrillat and Houziaux, 1967; Johnson, 1967).

History of Variations

The strong interest in γ Cas stems from the rather remarkable sequence of variations which the star exhibited during the 1930's. These spectral changes have yet to be completely explained, and they place γ Cas among the most unusual of the Be stars.

As has been briefly mentioned, from the mid-1800's until about 1929, γ Cas behaved like an ordinary stable Be star. During that time the star did exhibit a few very minor changes in brightness of less than $0^m.2$ (Edwards, 1956) as well as some variation in emission and shell absorption line visibility, but these were gradual changes over very limited range. The hydrogen emission V/R ratios were known to vary, but again, only over a very small amount, the value remaining very nearly unity.

In 1929, the spectrum began a series of rapid and very obvious changes. At first, the amplitude of the V/R fluctuations increased, and then in 1933 V/R rose very sharply, while at the same time the separation of the two components decreased steadily until there was only a single component with no central absorption (Edwards, 1956). Emission lines attributable to Fe II, Mg II, Si II, Ca II, and He I also appeared. These events continued throughout 1934, and by 1935 they began to disappear. The Balmer lines again showed two emission components, V/R reached a minimum, and the other emission faded.

That was not to be the end of this star's period of activity, however, for in mid-1936 Baize detected a $0^m.3$ increase in brightness (Heard, 1937) which, it developed, preceded another period of spectroscopic changes in 1937. The pattern for this second outburst was essentially the same as in 1933-34, with the hydrogen emission lines

again becoming single (Heard, 1938). At the time in 1937 when these single emission lines reached their greatest intensity the star also achieved its greatest luminosity, which was nearly one magnitude brighter than before the outburst (Edwards, 1956). During 1938, the emission lines again became double, V/R fell below unity, and the star became fainter. As in 1935, the end of this outburst was followed by the appearance of a shell spectrum, marked at first by the appearance of $\text{He I } \lambda 3889$ in absorption. This shell faded during 1940, but its disappearance was not uniform, as some of the shell absorption features would strengthen and fade erratically over one or two day intervals.

The final evidence of activity during this period was the development by the hydrogen emission lines of a structure more complex than the original two-component appearance (Edwards, 1956). Two new emission components appeared lying outside the original V and R components. A similar effect had also been briefly observed during the strong emission phase of 1937-38 (Burbidge and Burbidge, 1955), and was taken to indicate the presence of a new shell lying closer to the star and hence rotating faster than the previously observed emitting region. In both 1938 and 1940 these outer components gradually disappeared, and since 1940, γ Cas has remained relatively quiescent, exhibiting none of these dramatic, rapid spectral episodes.

The star has continued to show minor changes in spectral appearance, luminosity and spectral gradient, however, and recent observations by Hutchings (1967, 1970) indicate other short term changes in the Balmer emission lines themselves. He has observed profiles of $\text{H}\beta$ and $\text{H}\gamma$ with very high time resolution and finds them to be variable over time scales of a few minutes, while the separation and strength of the peaks

also at times varies over a few weeks. Hutchings states that, for observations from 1968 to 1969, he finds evidence for a 0.7-day period in the variation of separation and V/R ratio values for H β and H γ .

It will be recalled from Chapter 4 that no variations were found for the equivalent width in any of the four Balmer lines measured in γ Cas. More will be said of this result in the next section.

Significance of Variations

It is rather apparent from the foregoing summary of the variations of γ Cas that here is a star which at one time or another has exhibited nearly all of the types of Be variability which were discussed in Chapter 1, a fact which places it among the most interesting and potentially valuable of the Be stars. Its light variations and shell appearance during the 1930's have earned for it the classification as an irregular nova-like variable, and it also has shown V/R variation, change in emission component structure, and other profile variations. In accord with the reasoning of Chapter 1, it would appear that qualitative statements regarding the causes of some of these variations are possible, such as attributing the outburst of the 1930's to the eruptive formation of a shell which later dissipated, but the other changes pose more difficult problems. The short time scale fluctuations of profiles and short period variation of V/R ratio found by Hutchings are not yet clearly understood phenomena.

This observer would have expected to find equivalent width fluctuations also in this star, but over the four nights of observations there were none. It is, of course, possible that at other times the strengths of these lines do fluctuate and that these changes are not

continuous. Certainly it would have been interesting to have made similar observations during the activity of the 1930's. If, however, these Balmer lines of γ Cas are in fact constant in strength, it would seem that the mechanism of origin for the equivalent width variations is not directly related to those responsible for the types of variability which are observed in γ Cas.

φ PER HD 10516 HR 496

Published Spectral Types	References
B0 Ne	40
B1 pe (III-V) s.b.	8, 48, 75
B1 pe (III-IV)	26
B2 pe	9, 46
B2 V e	44

Published <u>V sin i</u> (km/sec)	References
550	69
560	2
530	12
450	73

General Spectroscopic Appearance

φ Per possesses a very pronounced Be shell type spectrum. The lower Balmer series members are marked by the typical emission feature divided into two components by a very deep central absorption core, all of which are superimposed upon a very broad absorption line. Also present in the spectrum are absorption features arising from helium and ionized metals such as iron and titanium. The strongest of the iron lines also have faint double emission cores. Photometrically there is also the infrared excess from Paschen emission such as found in γ Cas (Anrillat and Houziaux, 1967; Johnson, 1967).

History of Variations

Unlike γ Cas, the interest in φ Per does not arise from irregular,

violent changes in the spectrum such as the 1937 outburst, but rather from changes which occur in a periodic manner over an interval of 126.6 days. That time interval is the period of the radial velocity curve derived from the absorption cores of the hydrogen lines (Lockyer, 1926; Schiefer, 1936), although it is a very strange radial velocity curve indeed. (A very good graph of the curve is given by Hynek (1940), from whom the majority of this discussion is taken.) It is impossible to explain this radial velocity curve solely in terms of orbital motion, since no ellipse in any orientation will produce the observed secondary variations. One of the helium lines (specifically the singlet line λ 3965) shows the same curve as the hydrogen lines, while others (the triplet lines λ 4471 and λ 4026) show a velocity curve of opposite sign and without the secondary variations. In fact, the velocity curve from these lines looks very much like a well-behaved spectroscopic binary curve (Hendry, private communication).

Over the course of this 126.6^d period of radial velocities there are some interesting changes which occur in the appearance of the lines themselves. First, the hydrogen emission lines display a V/R variation which is periodic over the same interval (Ringuelet-Kaswalder, 1963), with the V/R maximum occurring at the time of maximum radial velocity (Hynek, 1940). Also varying over the same period are the widths of the emission components and the depth and width of the absorption cores of the hydrogen lines. Finally, the equivalent widths of the Balmer lines exhibit a variation curve very similar to the velocity curve but again without the secondary variations.

Besides the variations in the Balmer lines, there are other variations which occur during the radial velocity cycle. The calcium

H and K lines fluctuate in strength and at later parts of the cycle nearly disappear. Similarly, the helium triplet lines show cores of varying visibility.

Photometrically, φ Per has shown some brightness fluctuations on the order of from $0.^m 05$ to $0.^m 1$, but these are nonperiodic and apparently unrelated to the other changes described.

The results of Chapter 4 show that φ Per reveals more lines with real fluctuations in equivalent width than any other of the program stars, which adds even more interest to this very unusual star. The observations were made at 19-22 days into the 126.^d6 cycle and occur at a time when all velocity curves (hydrogen and helium) were at maximum value, and when the widths of the emission features were also at a maximum (Hendry, private communication).

Significance of the Variations

Since in φ Per we are most probably dealing with a spectroscopic binary consisting of two early B stars and having a period of 126.6 days (Hynek, 1940), and since the majority of changes which occur in the spectral features have periods of the same duration, it would appear that these variations are connected with the geometry of the binary system and represent effects of the position of the stars rather than any activity intrinsic to one or both of the stars themselves. For instance, the V/R changes may perhaps be attributed to the changing orientation of a gas stream (or streams) between the stars. The equivalent width fluctuations found in this study, however, must be the result of some other effect, for reasons discussed in Chapter 1.

φ Per has been determined to be a relatively massive binary system, with $M_1 \sin^3 i = 15 M_\odot$ and $M_2 \sin^3 i = 7.5 M_\odot$ (Batten, 1968),

and the primary also has a very high rotational velocity. It may be that this combination produces the conditions necessary to give rise to the random activity, be it flares, mechanical shocks, or electric or magnetic events, which can produce the observed fluctuations. Since these observations were taken at a phase of approximately 0.2 when both stars were moving in the line of sight and equally visible (except for possible gas streams), it is difficult to speculate as to which star (if not both) is undergoing the rapid activity. This is one case in which it would be particularly valuable to have observations of this type at many different phases of the orbit to determine whether the activity is visible at all relative positions of the stars.

28 TAU (Pleione) HD 23862 HR 1180

Published Spectral Types	References
B8 ne	40
B8 p (variable)	5, 41, 51, 75

Published <u>V sin i</u> (km/sec)	References
380	1
350	72, 73

General Spectral Appearance

Since the majority of Be stars are of spectral type B3 or earlier, Pleione at B8 is somewhat unusual even among Be stars. Also, there is evidence that the star is currently evolving off the main sequence toward the giant branch of the HR diagram (Ringuelet-Kaswalder, 1962; Struve and Wade, 1960).

Pleione is another of those stars with a shell spectrum episode in its history, and is similar to γ Cas but with a few important differences in the order of spectral events. When present, the shell spectrum with its wide Balmer emission components well divided and the absorption lines of ionized metals is very prominent. A significant point concerning these shell lines is that their profiles show rotational effects much stronger than effects due to ejection velocity of the shell from the star (Underhill, 1960), which implies a certain degree of stability in the shell structure. At other times the appearance is that of a rapidly rotating late B star with no or very faint emission in the Balmer lines. The star also shows the common infrared excess found in both γ Cas and η Per (Andrillat and Houziaux, 1967; Johnson, 1967).

History of Variations

Pleione, which is classified as an irregular eruptive variable in the General Catalogue of Variable Stars, began its shell episode in 1938. Previously, emission at the Balmer lines had been observed from 1888 to 1903 (no shell spectrum appeared), and it then disappeared until 1938 (Merrill, 1953). In 1939 the shell spectrum appeared, grew stronger until 1945-46, and then faded, being nearly gone by 1951. Note that this episode is significantly longer than any of the outbursts of γ Cas. Also unlike γ Cas, which experienced a sudden increase in brightness prior to developing a shell, Pleione reached a minimum brightness (about $0^m.4$ fainter than normal) in 1938, brightened slightly in 1942 and then reached a second minimum in 1945-46 when the shell absorption lines were the strongest and the ionization level in the shell was the lowest (Botsula and Sharov, 1959). Presumably the second minimum is due to obscuration by a large quantity of gas in the shell while the reason for the first is unclear.

In 1946, during the maximum of the shell strength, each successively higher Balmer line began showing a greater negative radial velocity, and this negative progression reached its greatest amount in 1951 as the shell was dissipating (Merrill, 1952). By 1953-54 the progression itself was also disappearing (Burd, 1954).

As for the other types of variations we have been discussing, it should be pointed out that Pleione does not show any variation of the V/R ratio in its emission lines (Ringuelet-Kaswalder, 1963). However, it is one star in which real fluctuations in equivalent width were found in H α and H β in the course of this research project.

Significance of the Variations

Just as in the case of γ Cas, it would seem that the appearance of the shell spectrum would indicate the development of some form of instability which caused the ejection of material from the stellar surface. As pointed out in Chapter 1, there is evidence that at least in the case of Pleione this ejection occurred slowly. Merrill (1952) feels the existence of the negative velocity progression in the Balmer lines indicates that the shell is formed by atoms leaving the photosphere slowly at first, and later being accelerated. Merrill and Lowen (1953) later present evidence indicating that shells around Be stars probably form slowly and that some shells become stable while others dissipate. Apparently γ Cas and Pleione both formed unstable shells, although in the latter star the duration of the shell episode coupled with the rotational profile visibility mentioned earlier indicates that Pleione's shell was much less unstable than that surrounding γ Cas. Perhaps this difference can eventually be traced to a difference in the nature or intensity of the generating mechanism.

The absence of V/R variations is interesting since real fluctuations in equivalent width now have been found in stars both with and without V/R variability. This would seem to indicate the lack of connection between the origin of the two phenomena, certainly not a surprising result in light of previous discussion concerning γ Cas.

48 PER HD 25940 HR 1273

Published Spectral Types References

B3 V pe	40, 44
B3 V (v)	58
B3 V p	8, 9, 17, 25, 30, 74
B3 e V	51

Published $V \sin i$ (km/sec) References

250	17, 74
210	13

General Spectral Appearance

48 Per is the one of the six program stars which has not shown a shell spectrum, but rather the simple Be characteristics. While the Balmer emission features are generally sharp, they do show some division into V and R components by a very shallow absorption core. The profiles, absence of shell lines, and the relatively low value for $V \sin i$ all indicate that 48 Per is viewed from very nearly pole-on.

History of Variations

48 Per has exhibited none of the eruptive events which, in the other program stars, led to the formation of a shell spectrum, but its spectrum has not been strictly constant, either. For example, Miczaika (1949) describes the appearance of the spectrum from September to mid-October, 1948, and in that interval the H β emission changed from double to single and back to double, and at the end of that period all Balmer

lines down to H λ 2 were double. Subsequently the emission was visible only to H δ , H β was double with V/R greater than unity, and this situation continued throughout all of 1949 (Miczaika, 1950). Since that time no other variations in the spectrum have been noted, except in the present study. 48 Per is the program star with the most obviously variable line, with the standard deviation from the mean of H α being greater than that for the comparison star on October 10 by a factor of 3.3.

Significance of the Variations

It is interesting that in this star which has shown the lowest amount of variability among all the six program stars should be found such a strikingly variable Balmer line strength in H α . Presumably the near pole-on orientation of the star precludes the visibility of other forms of variability which require the presence of the shell in the line of sight toward the star (for example, Huang's (1973) model of elliptical ring apsidal motion for V/R variability), if indeed these variations are occurring at all. The proposed explanation of flare- or shock-event origin of rapid equivalent width variability would not require such an orientation, however, making stars such as 48 Per equally good candidates for study as those with shell spectra. Certainly the results obtained here for 48 Per are encouraging that these stars may be the best candidates.

59 CYG HD 200120 HR 8047

Published Spectral Types	References
B3 ne	40
O9 V	7, 24
B0 p	28
B1 IV? e	26, 44, 46, 48, 60, 75

Published <u>V sin i</u> (km/sec)	References
450	2, 12
420	50

General Spectral Appearance

59 Cyg is classed as a shell star, but it is not at all the typical example of this type of spectrum. Butler and Thompson (1961) point out that in fact the spectrum, except for the Balmer emission, is practically featureless, and attribute this condition to the high rotation of the star which broadens the absorption lines so much as to wash them out. Morgan and Hansen (1946) found emission lines of Fe II (though variable in intensity over a few months and sometimes invisible) in the spectrum, and compared the spectral appearance to that of μ Per.

History of Variations

59 Cyg has undergone irregular brightness fluctuations which have caused it to be classed as an irregular eruptive variable in the General Catalogue of Variable Stars, but the star has not shown the

development of a strong shell spectrum with obvious sharp absorption lines as have, for example, γ Cas or Pleione. However, Merrill and Burwell (1949) report that from 1946 to 1948 the star underwent very large fluctuations in the V/R ratio (although V/R was always less than unity). They also note that the Balmer emission lines increased during this time period to the greatest strength ever observed for the star. So despite its nearly featureless spectrum, the star 59 Cyg is not without variability.

The present research project includes only one block of observations (of H β and H γ) for this star, and so while no variations in equivalent width were found, it is obvious that with this small amount of data there is the greatest amount of uncertainty whether other lines are variable or whether these lines are variable at other times.

Significance of the Variations

The irregular fluctuations in luminosity and the changing strength of Balmer and Fe II emission lines indicate that some form of eruptive activity is lifting material from the star. However, the fact that no strong shell spectrum has been observed implies that the quantity of ejected material must be small. The high value of rotation velocity shows that the axis of the star is highly inclined to the line of sight, and one would therefore expect to see the usual shell absorption spectrum if in fact a large amount of material were ejected from the star.

Since the V/R variations are not observed to be periodic or continuous it would appear that they are not connected with the apsidal motion of an elliptical ring, but rather most likely are related to the eruptive events of the star.

As mentioned, very few observations were made of this star during this project because of early evening cloud problems, and so it is difficult to say for certain that equivalent width fluctuations are not occurring. It would be very desirable in the future to make more extensive measurements of this star, for it would seem that this star with its eruptive activity might be a good candidate for the rapid activity such as has been suggested as the origin for the phenomenon being studied here.

o AND HD 217675 HR 8762

Published Spectral Types	References
B6.5 e	40
B6 p	44, 73
B6 +A2 p	26
B6 pe	69

Published <u>V sin i</u> (km/sec)	References
330	69, 74
360	2, 71
290	12
320	72

General Spectral Appearance

At this stage, rather than repeat the details of the spectral appearance, it is necessary only to say that this star is typical of stars such as γ Cas and Pleione which have at some time displayed a Be shell spectrum.

History of Variations

o And has actually passed through three shell episodes since 1890, specifically in 1890, 1920, and 1950 (Pasinetti, 1968a, 1968b). In 1903, 1933 and 1963 there was no shell spectrum, and in the intervening years there were faint absorption cores in the Balmer emission lines indicating the presence of a very thin shell.

Slettbak (1952) points out that from 1949 to 1952 there were changes in the emission structure of $\text{H}\alpha$ (an increase in the quantity

shown by further observations that these fluctuations are never seen in the star, it would indicate that whatever mechanism is responsible for these changes, it is not caused or intensified by the conditions found in this kind of close binary system. As in other cases, however, it is not possible to definitely conclude without further observations that the Balmer features are not experiencing equivalent width changes.

CONCLUSION

A. Summary of Results

We briefly summarize the results of the present research presented in detail in the foregoing chapters by calling attention to these main points:

1. In seven instances the existence of real fluctuations in the equivalent widths of Balmer lines in three stars from the program list has been determined.
2. The fluctuations have time scales on the order of from three to thirty minutes.
3. These variations amount to a few percent of the total line strength (except in those cases discussed in which the apparent percentages are probably artificially high).
4. The variations of any one line are not always present, and not all lines of any one star vary simultaneously, which perhaps is an effect of stratification in the shell such as observed in o And.
5. The fluctuations are nonperiodic.
6. The above facts taken together support the interpretation that the mechanism of origin of the phenomena is intermittent, random, and localized in a small region on the star. The most probable candidate for this mechanism would seem to be some form of flare activity causing bursts of radiation and perhaps a shock front to move through the circumstellar ring.

B. Comments on Improving the Present Research

Ways to improve a project usually suggest themselves after the analysis has been completed, and in the case of this program there is the matter of making only five observations of the comparison stars before and after each program star block. Despite the apparent stability of the IDS and the assumed constant equivalent widths of comparison star lines, it would have provided an even better check of the results to have lengthened the amount of time spent observing the comparison stars. The number of comparison observations was deliberately made small to allow the greatest number of program observations, but a longer time base on which to measure the comparison star values would perhaps have been valuable.

There is yet another advantage which could have been realized from having made comparison star observation blocks as long as those for program stars. These blocks could then have been put through the power spectrum analysis. Since the lines in these stars are assumed constant, these results would have given a more accurate estimate of the noise level in the power spectra, thus making the periodicity check even more precise.

C. Suggestions for Further Research

Several ideas for further observational and theoretical research in this area are suggested by the results of this project. It would be desirable to have some very long term monitoring of line strengths in these program stars as well as other Be and Be shell stars to determine answers to these questions:

1. Do all stars of these spectral types at some time undergo

such fluctuations, or are there in fact some which never do while others commonly exhibit the phenomenon?

2. Since the fluctuations of a given line are apparently not continuous, how long does one episode last?

3. Are the episodes periodic even though the fluctuations are not?

4. Are variations in some lines sometimes or always followed at a later time by variations in other lines of the same star, and if so, what is the interval?

Also very important would be theoretical consideration of the description of the actual conditions in the emitting regions during the fluctuations and of the likelihood that the flare or shock mechanism could produce the phenomenon.

REFERENCES

1. Abt and Hunter: 1962, Ap. J., 136, 381.
2. Andrillat and Houziaux: 1967, Journal Des Observateurs, 50, 107.
3. Archer: 1959, Observatory, 79, 99.
4. Bahng: 1971, Ap. J. (Letters), 167, L75.
5. Bappu, Chandra, Sanwal and Sinhval: 1962, M.N.R.A.S., 123, 521.
6. Batten: 1968, A. J., 73, 551.
7. Belyakina and Chugainov: 1959, Notices of the Crimean Astrophysical Observatory, No. 22, 25.
8. Blaauw: 1956, Ap. J., 123, 408.
9. Borgman: 1960, B.A.A.N., 15, 255.
10. Botsula and Sharov: 1959, Peremennye Zvezdy, 12, 398.
11. Bouique: 1957, Publications De L'Observatoire de Haute-Provence, 4, 52.
12. Boyartchuk: 1957, Soviet Astronomy, 1, 192.
13. Boyartchuk and Pronik: 1964, Notices of the Crimean Astrophysical Observatory, 31, 3.
14. Burbidge and Burbidge: 1951, Ap. J., 113, 84.
15. Burbidge and Burbidge: 1955, Observatory, 75, 256.
16. Burd: 1954, P.A.S.P., 66, 208.
17. Butler and Seddon: 1960, Publications of the Royal Observatory, Edinburgh, 2, No. 5.
18. Butler and Thompson: 1961, Publications of the Royal Observatory, Edinburgh, 2, 225.
19. Copeland and Heard: 1963, Publications of the David Dunlap Observatory, 2, 317.
20. Cowley and Gugula: 1973, Astronomy and Astrophysics, 22, 203.
21. Cowley and Marlborough: 1968, P.A.S.P., 80, 42.
22. Delplace: 1970, Astronomy and Astrophysics, 7, 459.

23. Divan: 1954, Annales D'Astrophysique, 17, 456.
24. Edwards: 1956, Vistas in Astronomy, ed. Beer (New York: Pergamon Press), 2, 1470.
25. Feast, Thackaray and Wesselink: 1955, Mem. R.A.S., 67, 51.
26. General Catalogue of Variable Stars: 1969 (Moscow: Sternberg State Astronomical Institute of Moscow State University).
27. Gray and Marlborough: 1974, Ap. J. Supplement, 27, 121.
28. Hack: 1953, Annales D'Astrophysique, 16, 417.
29. Hack and Struve: 1971, Stellar Spectroscopy -- The Peculiar Stars, (Trieste: Osservatorio Astronomico Trieste).
30. Harris: 1956, Ap. J., 123, 371.
31. Heard: 1937, J. R. A. S. Canada, 31, 60.
32. Heard: 1938, J. R. A. S. Canada, 32, 353.
33. Hendry, private communication.
34. Hoag, Ball and Trumbo: 1971, Publication of the Royal Observatory, Edinburgh, 8, 71.
35. Huang: 1973, Ap. J., 183, 541.
36. Hutchings: 1967, Observatory, 87, 289.
37. Hutchings: 1970, M.N.R.A.S., 150, 55.
38. Hutchings: 1972, New Directions and New Frontiers in Variable Star Research, Proc. IAU Colloq. No. 15 (Bamberg: Astronomisches Institut der Universitat Erlangen-Nurnberg), 279.
39. Hynek: 1940, Contributions of the Perkins Observatory, No. 14.
40. Jaschek, Ferrer and Jaschek: 1971, Observatorio Astronomico De La Universidad Nacional De La Plata Serie Astronomicia, 37.
41. Johnson: 1953, Ap. J., 118, 370.
42. Johnson: 1955, Observatory, 75, 68.
43. Johnson: 1967, Ap. J., 150, L39.
44. Kopylov: 1958, Notices of the Crimean Astrophysical Observatory, No. 20, 156.
45. Limber: 1970, Stellar Rotation (IAU Colloquium) ed. Slettebak (New York: Gordon and Breach), 274.

46. Ljunggren and Oja: 1961, Uppsala Astronomiska Observatorium Annaler, 4, No. 10.
47. Lockyer: 1926, M.N.R.A.S., 86, 474.
48. Lynds: 1959, Ap. J., 130, 577.
49. McLaughlin: 1961, J.R.A.S. Canada, 55, 13.
50. Meisel: 1968, A. J., 73, 350.
51. Mendoza: 1956, Ap. J., 123, 54.
52. Merrill: 1952, Ap. J., 115, 145.
53. Merrill: 1953, P.A.S.P., 65, 113.
54. Merrill and Burwell: 1949, Ap. J., 110, 387.
55. Merrill and Lowen: 1953, Ap. J., 118, 18.
56. Miczaika: 1949, Astronomische Nachrichten, 277, 167.
57. Miczaika: 1949, Astronomische Nachrichten, 279, 19.
58. Miczaika: 1951, Z. fur Astrophysik, 29, 262.
59. Miller: 1954, Ap. J., 120, 265.
60. Morgan, Code and Whitford: 1955, Ap. J. Supplement, 2, 41.
61. Morgan and Hansen: 1946, Ap. J., 103, 379.
62. Morgan, Keenan and Kellman: 1943, Atlas of Stellar Spectra.
63. Osterbrock: 1957, Ap. J., 125, 622.
64. Pasinetti: 1968a, Contributi Dell'Osservatorio Astronomico Di Milano-Merate, No. 276.
65. Pasinetti: 1968b, Contributi Dell'Osservatorio Astronomico Di Milano-Merate, No. 283.
66. Pecker: 1953, Annales D'Astrophysique, 16, 321.
67. Ringuelet-Kaswalder: 1962, Boletin De La Asociacion Argentina De Astronomia, No. 2, 48.
68. Ringuelet-Kaswalder: 1963, P.A.S.P., 75, 323.
69. Sandage: 1955, Ap. J., 122, 263.
70. Schiefer: 1936, Ap. J., 84, 568.

71. Slettebak: 1952, Ap. J., 115, 573.
72. Slettebak: 1966a, Ap. J., 145, 121.
73. Slettebak: 1966b, Ap. J., 145, 126.
74. Slettebak and Howard: 1955, Ap. J., 121, 102.
75. Stebbins and Kron: 1955, Ap. J., 123, 440.
76. Stock: 1956, Ap. J., 123, 253.
77. Struve: 1931, Ap. J., 73, 94.
78. Struve and Wade: 1950, Observatory, 80, 229.
79. Taffara: 1959, Memorie Della Societa Astronomica Italiana, 30, 135.
80. Underhill: 1960, Contributions of the D.A.O., No. 68.
81. Underhill: 1966, The Early Type Stars (Dordrecht: D. Reidel Publishing Co.), 226.

Table 1

PROGRAM AND COMPARISON STARS

<u>Name</u>	<u>Spectral Type</u>	<u>Binary Data</u>	<u>Variable Data</u>	<u>Comparison Star</u>	<u>Spectral Type</u>
γ Cas HD 5394 HR 264	B0 IV? e (shell)	2 visual companions 1 not definite	Irregular Nova-like	ν And HD 4727 HR 226	B5 V
ω Per HD 10516 HR 496	B1 III-IV? pe (shell)	Spectroscopic Binary (126.6-day period)		ν And HD 4727 HR 226	B5 V
ζ 28 Tau Pleione HD 23862 HR 1180	B8 p (shell)		Irregular Eruptive	34 Per HD 21428 HR 1044	B5 V
48 Per HD 25940 HR 1273	B3 V pe			34 Per HD 21428 HR 1044	B5 V
59 Cyg HD 200120 HR 8047	B1 IV? e (shell)	3 visual companions	Irregular Eruptive	57 Cyg HD 199081 HR 8001	B5 V
ο And HD 217675 HR 8762	B6p + A2 (shell)	β Lyrae type eclipsing (1.6-day period)		ν And HD 4727 HR 226	B5 V

Table 2

PROGRAM STAR BLOCK MEAN EQUIVALENT WIDTHS

Star	Line	Date (10/72)	No. of Scans	No. of Observations	Mean Eq. Width (A)	Published Eq. Width (A)	(Ref.)
γ Cas	H α	10	1000	91	-26.7		
	H α	11	1000	115	-26.7		
	H δ	10	1000	91	0.1		
	H δ	11	1000	115	0.1	1.4	
	H β	9	700	100	-2.8		76
	H β	12	500	205	-2.5	1.0	
	H γ	9	700	100	0.2		
	H γ	12	500	205	0.1	0.8	
	H α	10	1000	99	-53.4		
	H α	11	1500	90	-53.2		
ω Per	H δ	10	1000	99	1.5		
	H δ	11	1500	90	1.6		
	H β	9	1000	75	-3.7		
	H β	12	1000	115	-3.2		
	H γ	9	1000	75	1.2		
	H γ	12	1000	115	1.5		

Table 2 (Continued)

Star	Line	Date (10/72)	No. of Scans	No. of Observations	Mean Eq. Width (Å)	Published Eq. Width (Å)	Published Eq. Width (Ref.)
28 Tau	H α	10	1000	60	- 1.0		
	H α	11	1500	75	- 1.3		
	H δ	10	1000	60	6.0		
	H δ	11	1500	75	6.0	6.4	
	H β	9	--	--	--		
	H β	12	1500	75	6.4	5.7	
	H γ	9	--	--	--		
	H γ	12	1500	75	6.0	6.6	
48 Per	H α	10	1000	45	-17.6		
	H α	11	1000	55	-17.4	-16.6	
	H δ	10	1000	45	4.9		
	H δ	11	1000	55	4.7	4.8	
	H β	9	1000	60	3.1		
	H β	12	1000	70	3.3	3.9	
	H γ	9	1000	60	4.7		
	H γ	12	1000	70	4.8	5.4	

Table 2 (Continued)

Star	Line	Date (10/72)	No. of Scans	No. of Observations	Mean Eq. Width (Å)	Published Eq. Width (Å)	Published Eq. Width (Ref.)
o And	H α	10	--	--	--		
		11	1000	60	4.4	4.5	
	H δ	10	--	--	--		
		11	1000	60	4.6	4.9	
	H β	9	1000	57	5.0		64
		12	1000	60	5.3	6.6	
	H γ	9	1000	57	4.9		
		12	1000	60	4.9	5.6	
	H β	9	1000	60	1.2		
	H γ	9	1000	60	3.0	2.6	16

Table 3

COMPARISON STAR BLOCK MEAN EQUIVALENT WIDTHS

Star	Line	Date (10/72)	Mean Eq. Width (Å)	Published Eq. Width (Å)	(Ref.)
HR 226	H α	10	5.9		
		11	5.7		
	H δ	10	6.6		
		11	6.4	6.4	44
	H β	9	7.0		
		12	6.9	6.6	
	H γ	9	7.0		
		12	6.9	7.5	
HR 1044	H α	10	5.4		
		11	5.4		
	H δ	10	6.1		
		11	5.8		
	H β	9	6.5		
		12	6.6		
	H γ	9	6.4		
		12	6.3		
HR 8001	H β	9	7.0		
		9	6.6	6.1	44
	H γ				

Table 4

PROGRAM TO COMPARISON STAR STANDARD DEVIATION RATIOS

Star	Line	Date (10/172)	σ_p (A)	σ_{c1} (A)	σ_{c2} (A)	$\frac{1}{2} \left(\frac{\sigma_p}{\sigma_{c1}} + \frac{\sigma_p}{\sigma_{c2}} \right)$
γ Cas	H α	10	0.41	0.26	0.30	1.5
		11	0.31	0.35	0.29	1.0
	H δ	10	0.25	0.16	0.14	1.7
		11	0.13	0.15	0.23	1.0
	H β	9	0.13	0.23	0.48	0.4
		12	0.11	0.37	0.15	0.5
	H γ	9	0.12	0.09	0.14	1.1
		12	0.0	0.20	0.18	0.4
ω Per	H α	10	0.56	0.30	0.44	1.6
		11	0.66	0.29	0.24	2.5
	H δ	10	0.33	0.14	0.13	2.4
		11	0.19	0.23	0.31	0.7
	H β	9	0.20	0.48	0.27	0.6
		12	0.17	0.15	0.08	1.6
	H γ	9	0.29	0.14	0.15	2.0
		12	0.22	0.18	0.03	2.0

Table 4 (Continued)

Star	Line	Date (10/172)	σ_p (Å)	σ_{c1} (Å)	σ_{c2} (Å)	$\frac{1}{2} \left(\frac{\sigma_p}{\sigma_{c1}} + \frac{\sigma_p}{\sigma_{c2}} \right)$
28 Tau	H α	10	0.55	0.38	0.20	2.1
		11	0.40	0.18	0.33	1.7
	H δ	10	0.27	0.19	0.11	1.9
		11	0.27	0.27	0.25	1.0
	H β	9	--	--	--	--
		12	0.38	0.12	0.38	2.1
	H γ	9	--	--	--	--
		12	0.21	0.27	0.14	1.1
	H α	10	0.38	0.20	0.08	3.3
		11	0.34	0.33	0.35	1.0
48 Per	H δ	10	0.18	0.11	0.22	1.2
		11	0.20	0.25	0.17	1.0
	H β	9	0.25	0.36	0.17	1.1
		12	0.23	0.38	0.24	0.8
	H γ	9	0.14	0.18	0.17	0.8
		12	0.11	0.14	0.19	0.7

Table 4 (Continued)

Star	Line	Date (10/172)	σ_p (Å)	σ_{c1} (Å)	σ_{c2} (Å)	$\frac{1}{2} \left(\frac{\sigma_p}{\sigma_{c1}} + \frac{\sigma_p}{\sigma_{c2}} \right)$
o And	Hα	10	--	--	--	--
	Hα	11	0.30	0.35	0.35	0.9
	Hβ	10	--	--	--	--
	Hβ	11	0.16	0.15	0.15	1.1
	Hγ	9	0.25	0.23	0.23	1.1
	Hγ	12	0.22	0.37	0.37	0.6
	Hγ	9	0.12	0.09	0.09	1.3
	Hγ	12	0.12	0.20	0.20	0.6
	Hβ	9	0.34	0.23	0.45	1.0
	Hγ	9	0.26	0.28	0.22	1.1

Table 5
LINES WITH REAL RAPID FLUCTUATIONS

Star	Line	Date (10/72)	$(\sigma_p / \bar{W} \cdot 100)$
ω Per	H α	11	1.2
	H δ	10	22.0
	H γ	9	24.2
	H γ	12	14.7
28 Tau	H α	10	55.0
	H β	12	5.9
48 Per	H α	10	2.2

Table 6
LINES WITH BORDERLINE RAPID FLUCTUATIONS

Star	Line	Date (10/'72)
φ Per	Hβ	12
28 Tau	Hα	11
28 Tau	Hδ	10

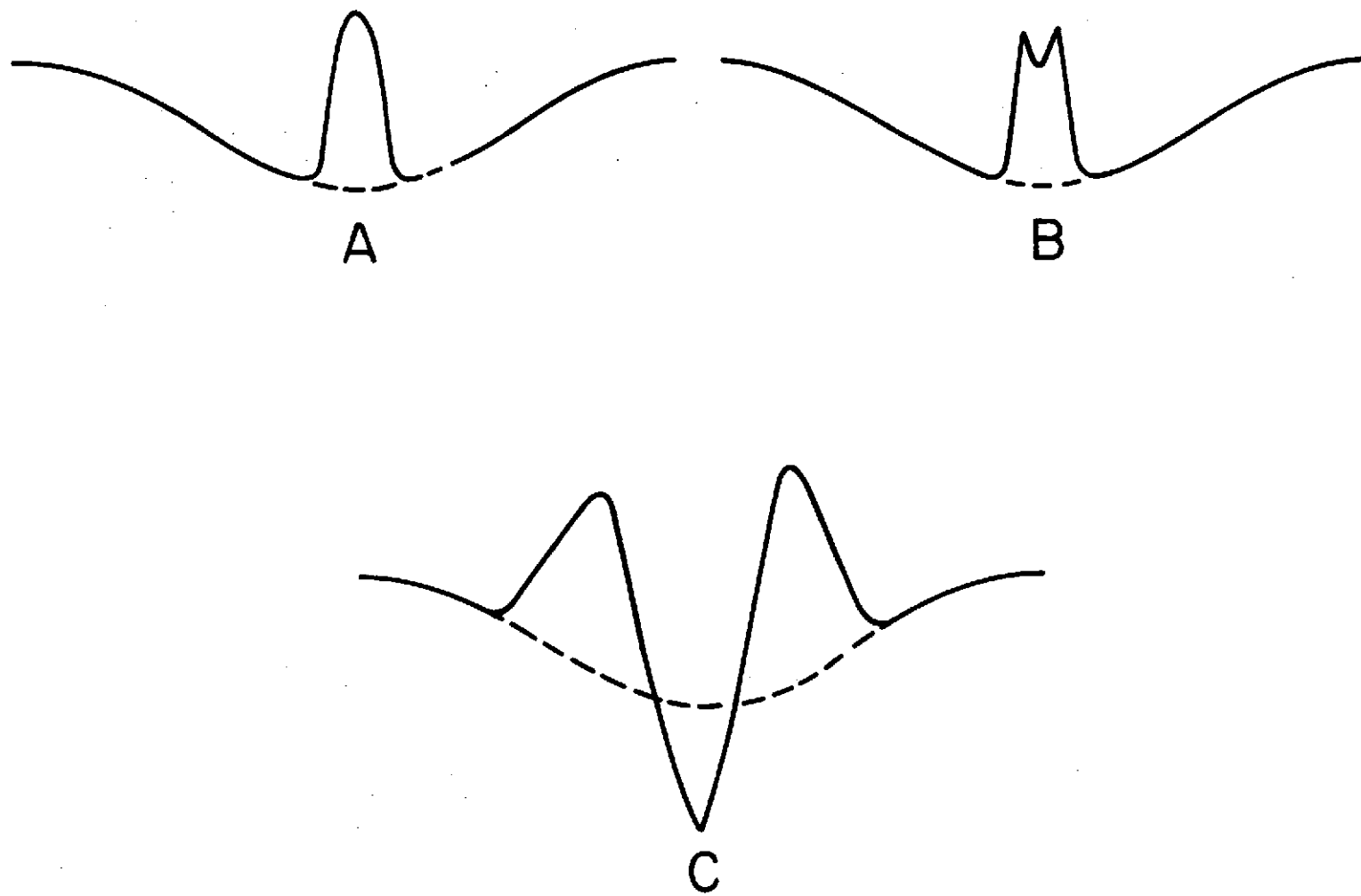


Fig. 1 Be AND Be SHELL HYDROGEN LINE PROFILES

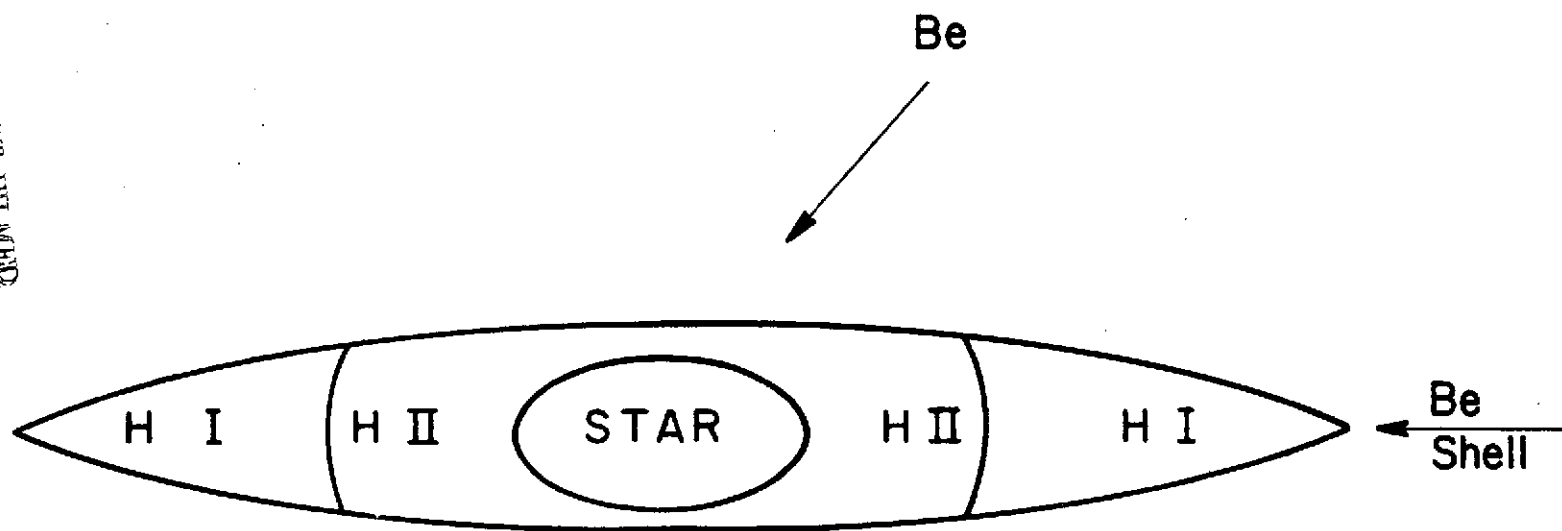


FIG. 2 LINE OF SIGHT ORIENTATION FOR Be AND Be SHELL SPECTRUM

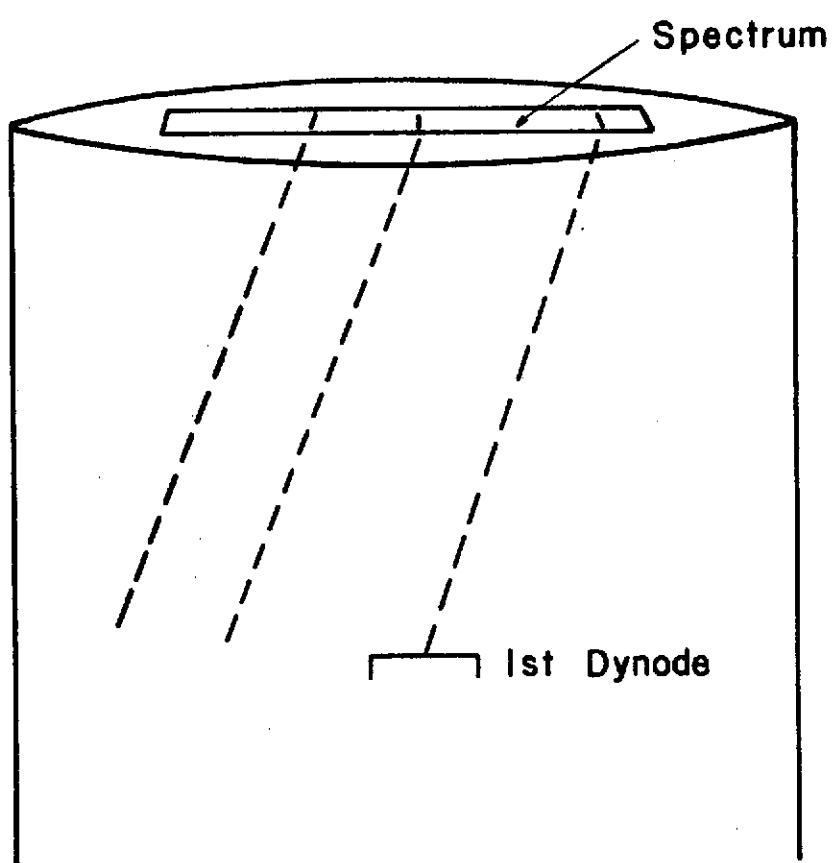


FIG. 7 SCHEMATIC ILLUSTRATION OF IMAGE DISSECTOR PRINCIPLE

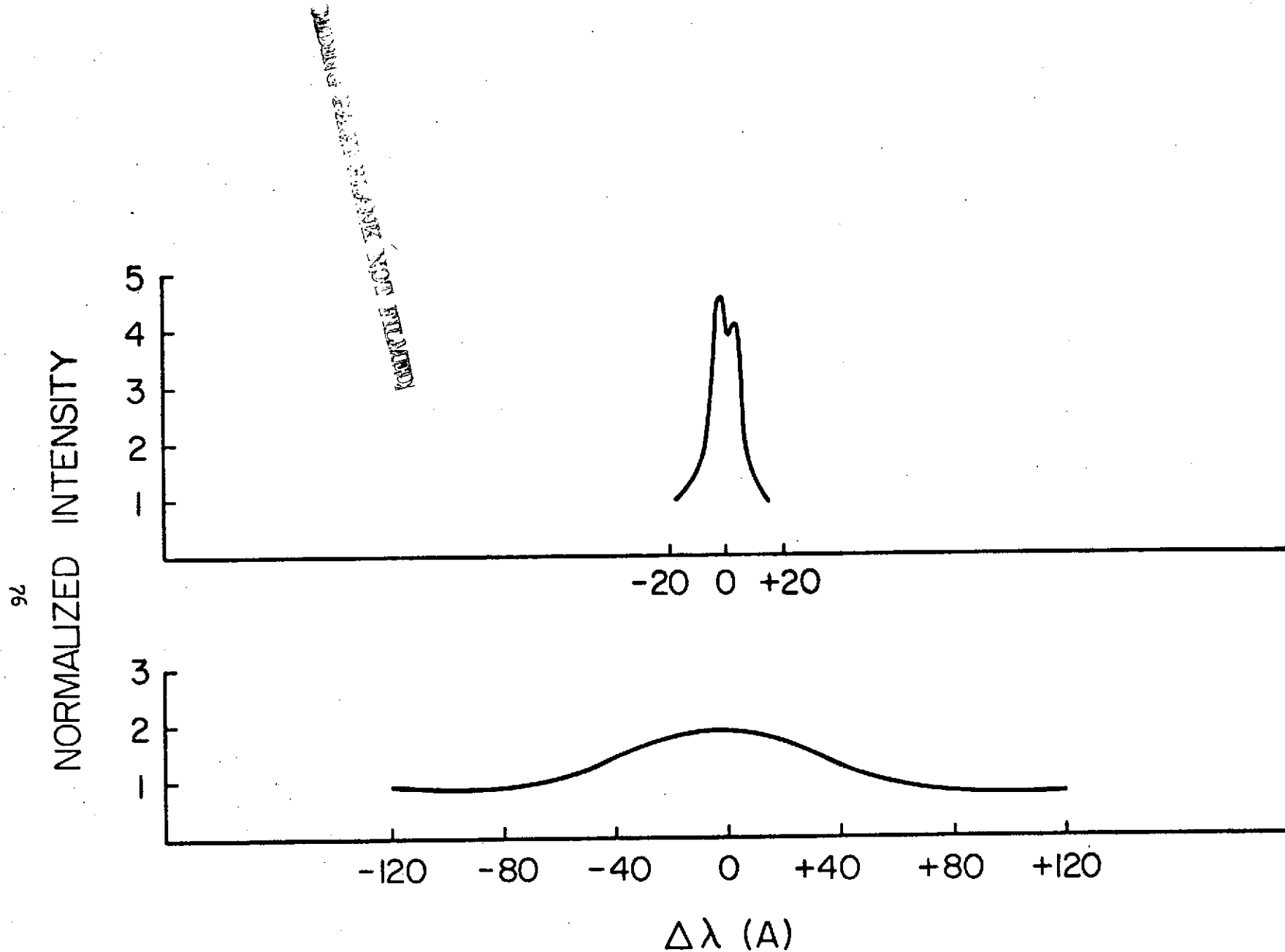


Fig. 4 EFFECT OF LOW SPECTRAL RESOLUTION ON OBSERVED LINE PROFILE

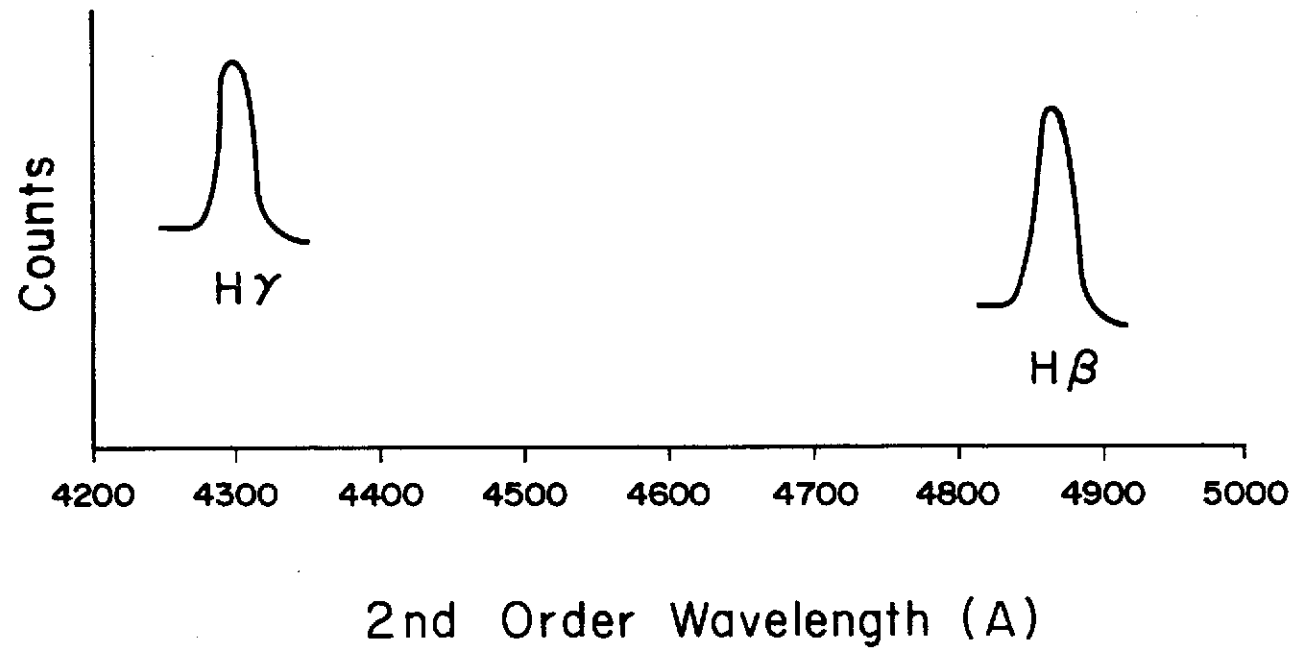


FIG. 5 SCANNING REGIONS FOR $H\beta$ AND $H\gamma$

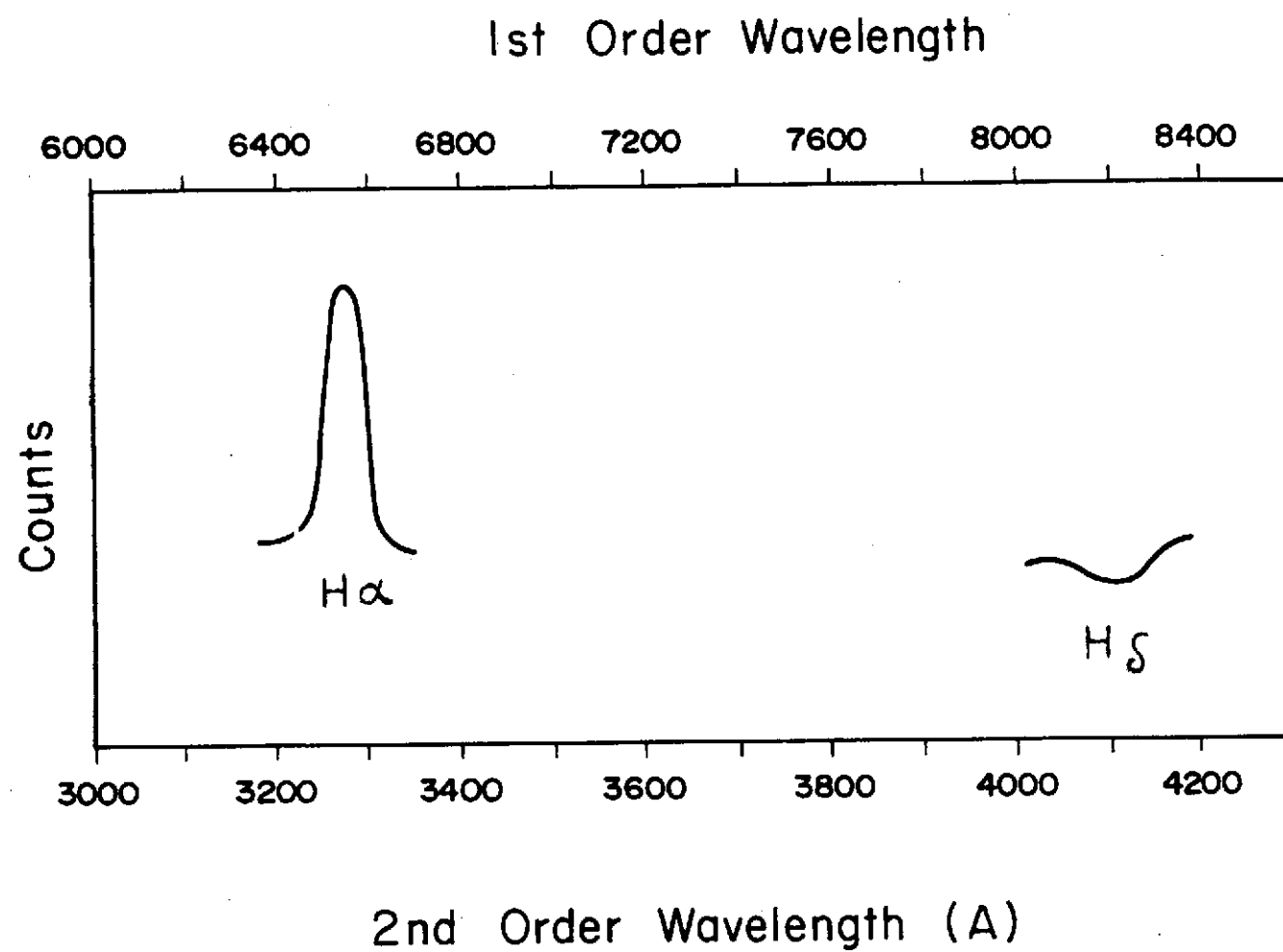


Fig. 6 SCANNING REGIONS FOR H α AND H γ

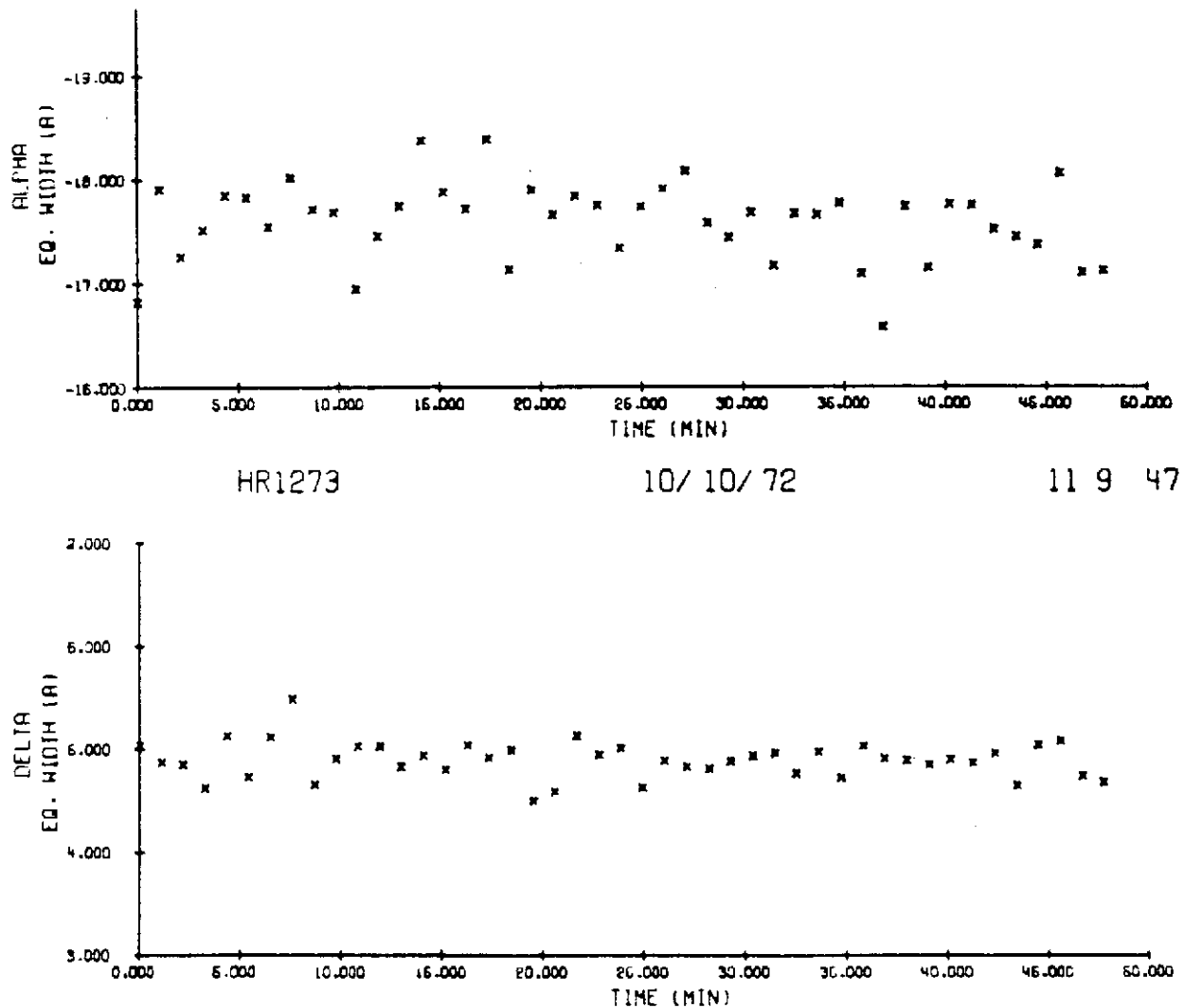


Fig. 7 GRAPH OF EQUIVALENT WIDTH VS TIME FOR 43 PER, H_α AND H_δ,
10 OCTOBER 1972 (UT)

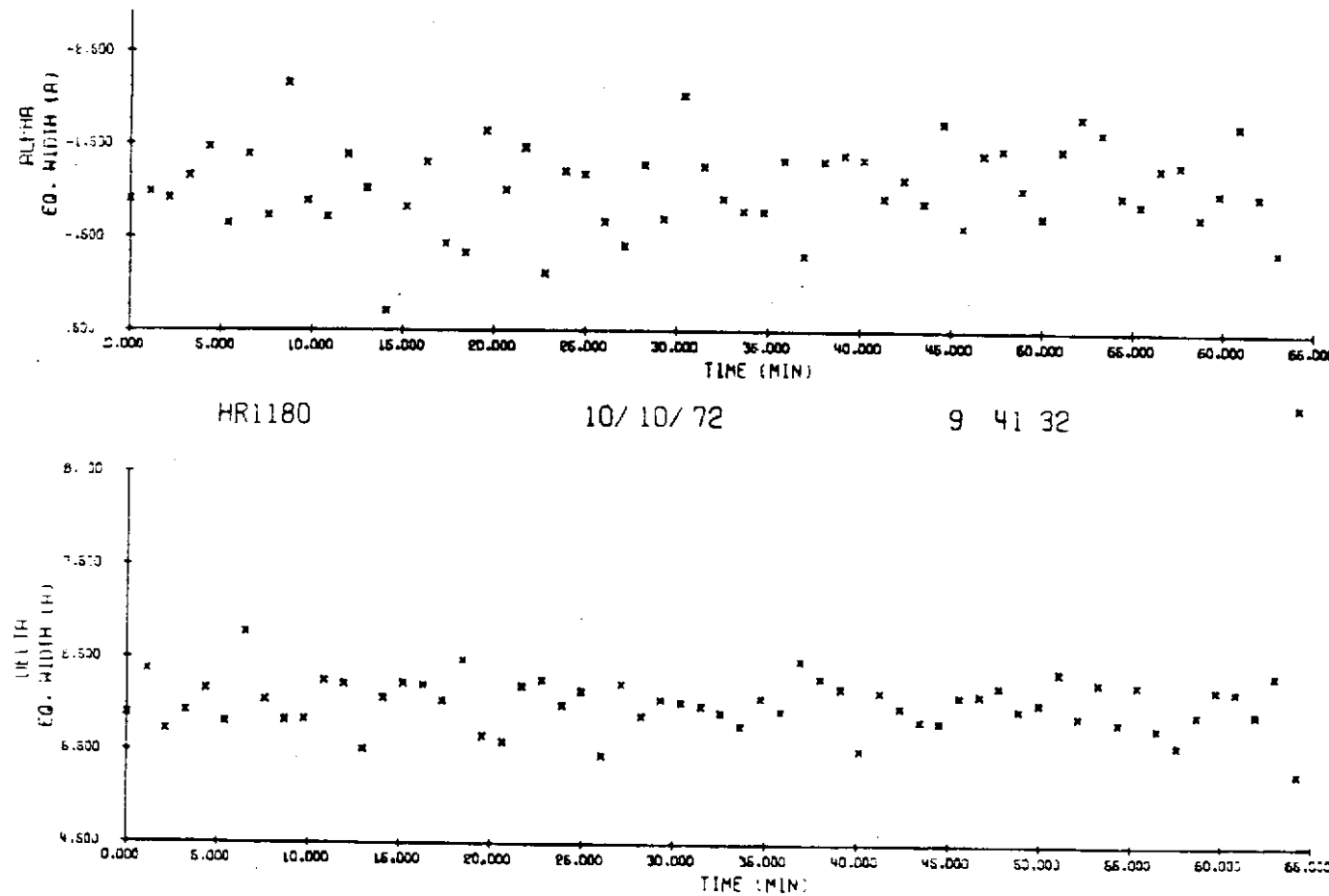
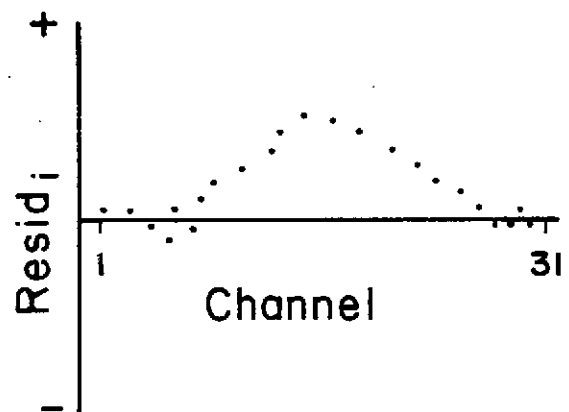
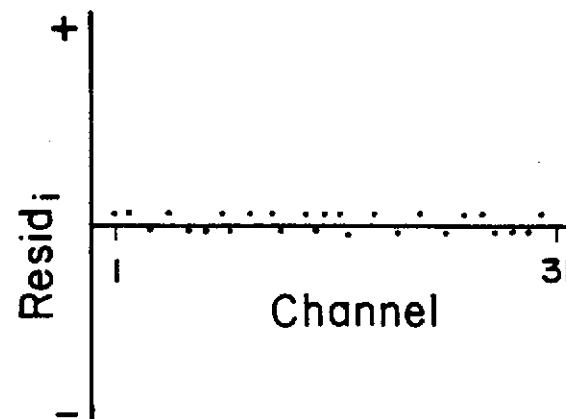


Fig. 8 GRAPH OF EQUIVALENT WIDTH VS TIME FOR 28 TAU, H α AND H γ ,
10 OCTOBER 1972 (UT)



Variable Profile



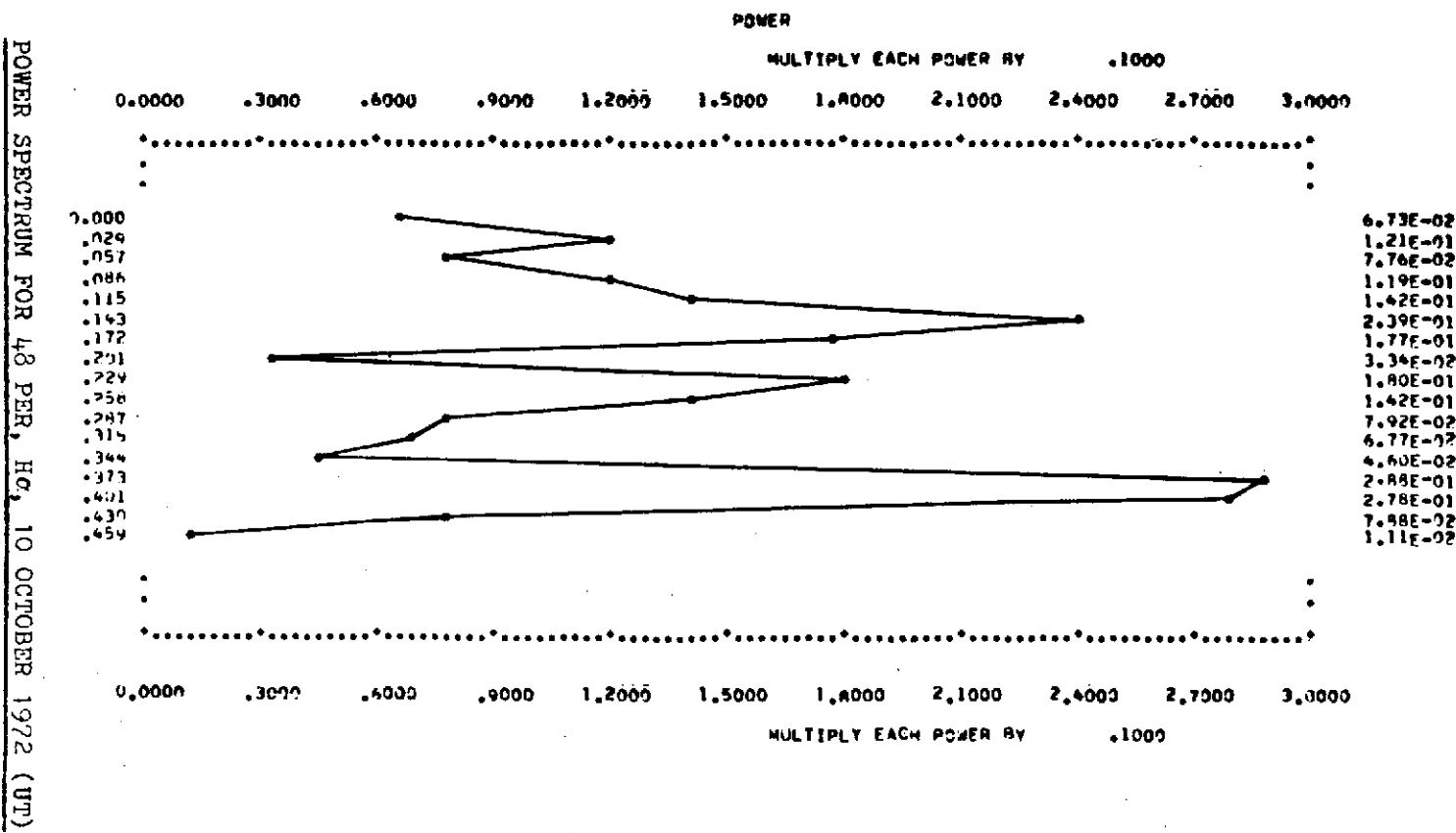
Nonvariable Profile

Fig. 9 EXPECTED GRAPH OF RESIDUAL PROFILES FOR A
VARIABLE AND NONVARIABLE OBSERVATIONAL LINE PROFILE

FIG. 10 POWER SPECTRUM FOR 48 PER, HO, 10 OCTOBER 1972 (UT)

Abscissa: Frequency (min^{-1})

Ordinate: Power



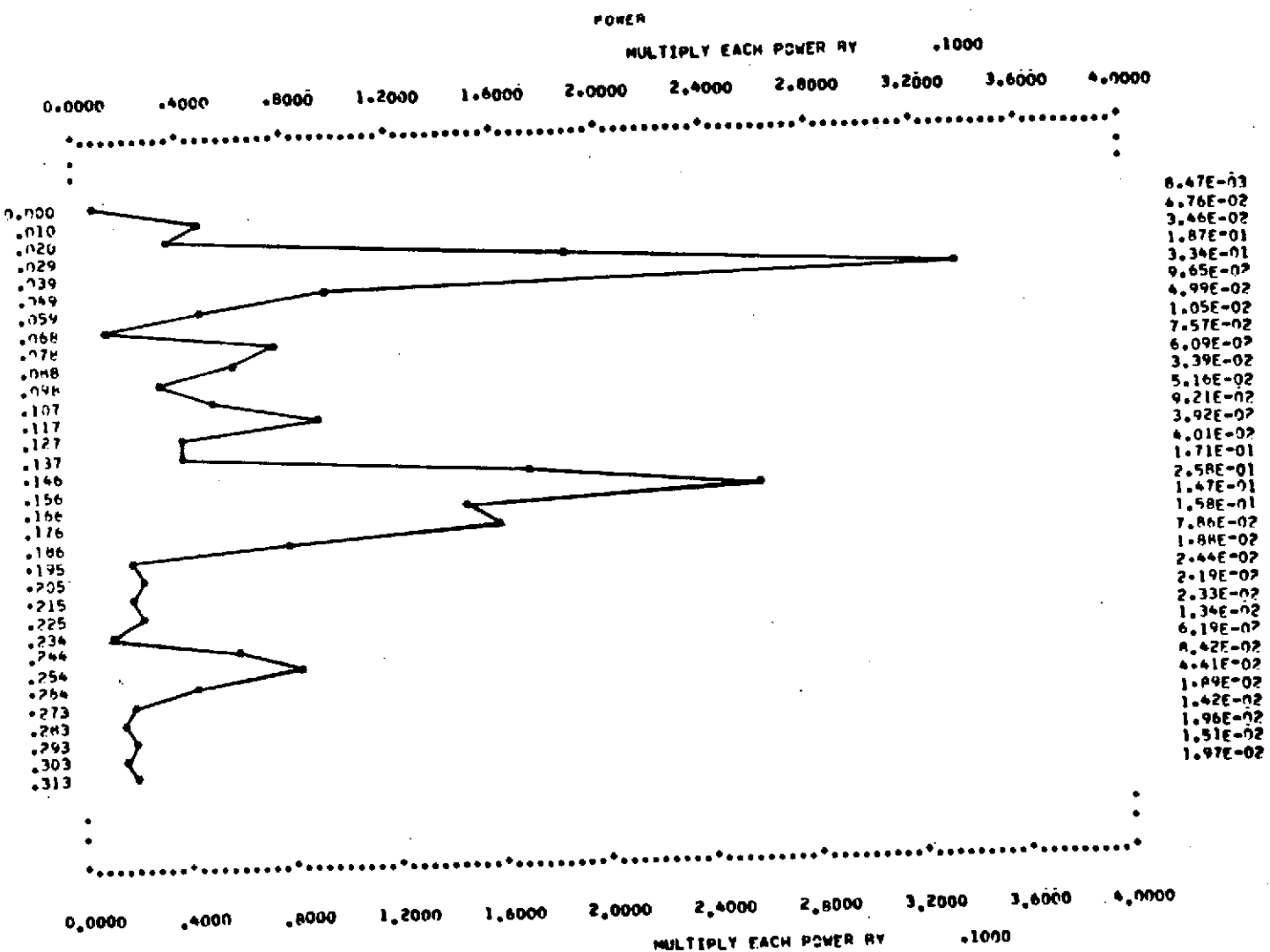


Fig. 11 POWER SPECTRUM FOR 28 TAU, Hy, 12 OCTOBER 1972 (UT)

Abscissa: Frequency (min⁻¹)
 Ordinate: Power

REPRODUCIBILITY OF THIS
 REPRODUCED PAGE IS POOR
 REFER TO PAPER COPY OF THIS

ORIGINAL PAGE IS POOR

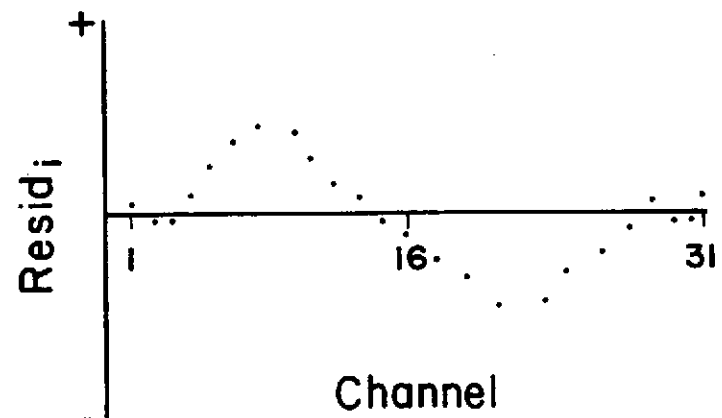
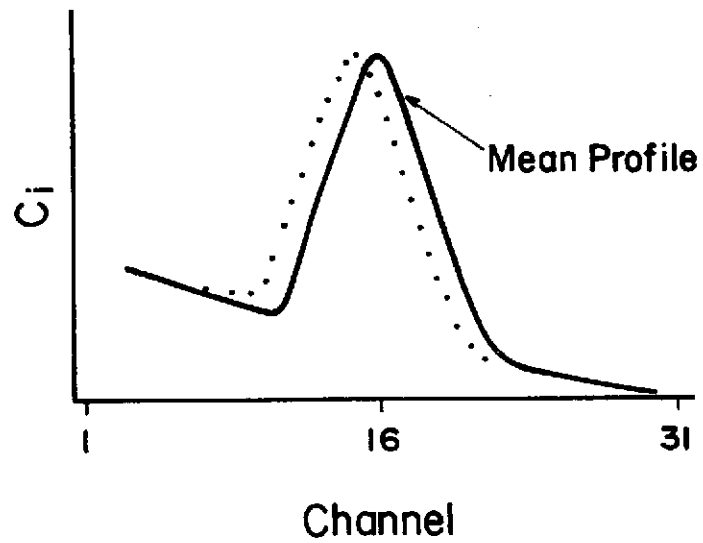


FIG. 11. EFFECT OF IDC CHANNEL POSITION INSTABILITY ON RESIDUAL LINE PROFILE

HR 1273

10/10/72

H DELTA

H ALPHA

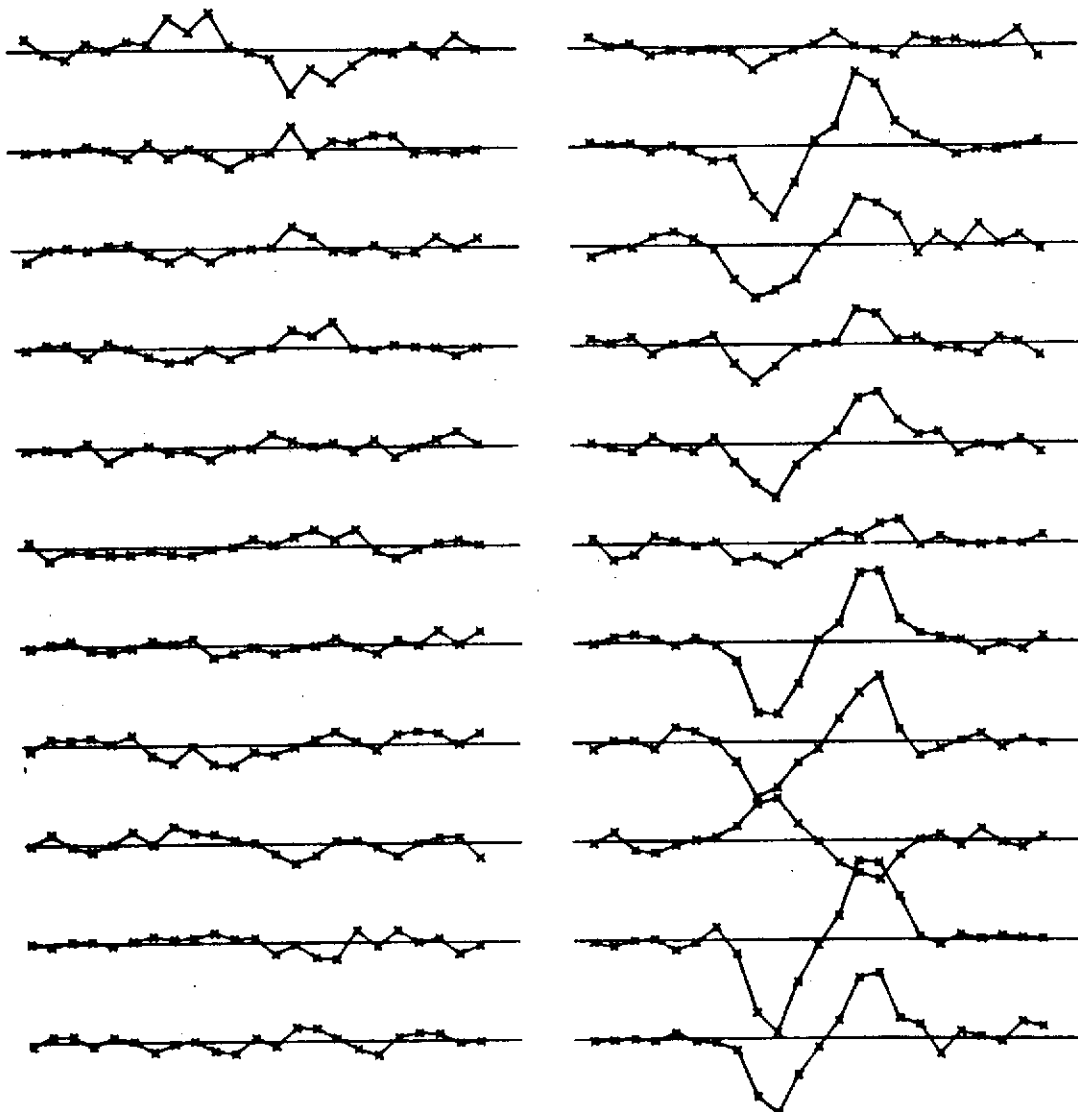


FIG. 13 GRAPH OF RESIDUAL PROFILES FOR 48 PER, H_α,
10 OCTOBER 1972 (UT)

Vertical separation of lines equals a 10% residual.

HR 1044

10/10/72

H DELTA

H ALPHA

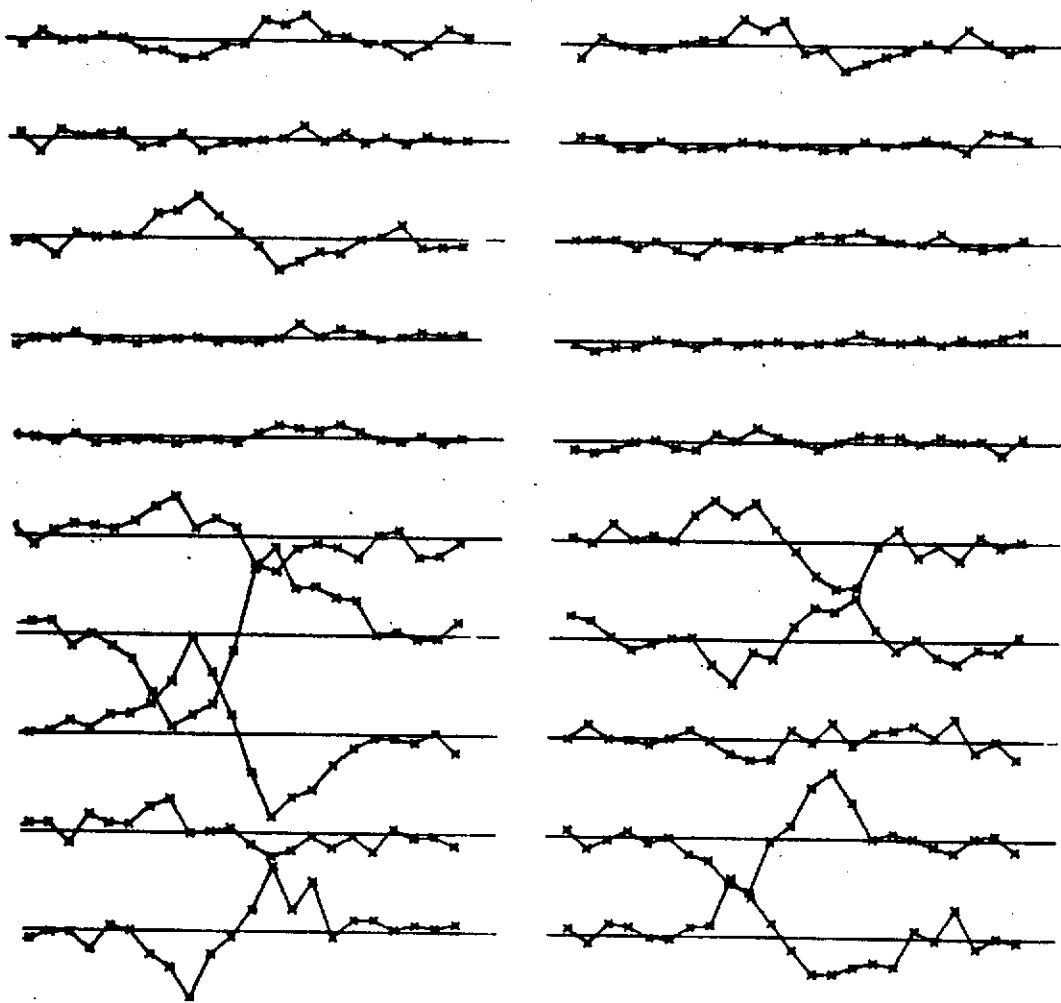


Fig. 14. GRAPH OF RESIDUAL PROFILES FOR 34 PER, H α ,
10 OCTOBER 1972 (UT)

Vertical separation of lines equals a 10% residual.